Lipophilic Metal−Salicylideneimine−Crown Ether Hybrids — Ditopic Carriers in the Facilitated Transport of Amphiphilic Molecules Across Bulk Liquid Membranes

Jay D. Pike,[a] Dell T. Rosa,[a] and Dimitri Coucouvanis*[a]

Keywords: Supramolecular chemistry / Molecular recognition / Manganese / Macrocyclic ligands / Facilitated transport

The crown ether-functionalized Mn^{III} salicylaldimine complexes manganese(III) 4,5-bis(3,5-di-*tert*-butylsalicylideneimine)benzo-18-crown-6-X [X = Cl^-, I^-, CH_3COO^-, $(CH_3)_3CCOO^-$, $B(Ph)_4^-$] have recently been synthesized and studied as effective ditopic transport carriers of hydrophobic amino acids and neurotransmitters through $CHCl_3$ bulk liquid membranes (BLMs). A detailed analysis of the BLM transport of tryptophan and serotonin with these complexes, along with various derivatives, shows the ditopic nature of the mechanism of transport and reveals the importance of the role of both the crown ether function and the metal center. Kinetic data on the BLM transport of tryptophan follow Michaelis–Menten behavior with K_m = 25 mM and $V_m = 6.75 \times 10^{-3} h^{-1}$. Variable temperature studies on the rate of transport of tryptophan (and serotonin) were conducted. From Arrhenius plots, the activation energies, E_a, and pre-exponential factors, A, were determined to be 20 ± 1 (17 ± 5) kJ mol^{-1} and 8200 (947) $M^{-1}h^{-1}$, respectively. From these parameters, values for the thermodynamic activation energies, $\Delta G^{\ddagger}$, $\Delta H^{\ddagger}$, and $\Delta S^{\ddagger}$ were calculated to be 26 ± 4 (32 ± 1) kJ mol^{-1}, 17 ± 1 (14 ± 5) kJ mol^{-1}, and –30 ± 9 (–60 ± 14) J K^{-1} mol^{-1}, respectively. Similar studies with serotonin are reported.

Introduction

Cell membranes that protect the cell and at the same time allow for the transport of solutes across the cell boundary consist of lipid bilayers that contain a hydrophobic interior flanked by hydrophilic surfaces. The transport of biologically important small molecules through cell membranes is an essential process for living organisms.[1] The vast majority of such molecules are water-soluble species that by themselves are insoluble in lipid membranes.

In the absence of sufficient hydrophobicity, facilitated transport by specific carriers is necessary to allow for appreciable partitioning for the transport of hydrophilic molecules.[2] A great number of naturally occurring carriers are known for the transport of amino acids, neurotransmitters, nucleosides, sugars, etc. Often these carriers are proteins of mostly unknown structures that exhibit high specificity in the recognition of substrates.[3] The transporter proteins are difficult to isolate, although several have been obtained from various systems including the *E. coli* glucose transport system,[4] the *E. coli* β-galactoside transport system,[5] the baker's yeast galactose transport system,[6] the *E. coli* leucine binding membrane component,[7] and the *E. coli* arginine transport system.[8]

Other hydrophilic molecules, including most drugs, cannot readily cross lipid bilayer membranes unassisted. Carriers for the facilitated transport of hydrophilic drugs across cell membranes are rare and the design and synthesis of such molecules are of vital concern to pharmacology.

The transport of particles across membranes may be either by simple passive permeation (free diffusion) or by facilitated diffusion. Facilitated transport may be "active" or "passive." In the former, the transport process is coupled with the free energy of a chemical reaction that takes place in the transport region and is converted into "pumping" work. In the latter, the driving force is derived from the concentration gradient across the membrane (electrochemical potential gradient) and is at times assisted by "counterflow". This occurs when concentration gradients of two substances at opposite sites of the membrane accelerate the rate of transport of both substances.[9] An example of this type of amino acid transport is the transport of the essential extracellular serine, glycine, and threonine in *Streptococcus faecium*. The transport of these amino acids into the cell is coupled with the outward transport of alanine, which is synthesized in large quantities inside the cells.[10]

Numerous artificial transport systems with varying degrees of success have been developed, including: a) the effective transport of amino acid derivatives by metal complex carriers across CH_2Cl_2 or $CHCl_3$ bulk liquid membranes (BLMs) using hydrophobic, neutral $LM(Cl)_2$ complexes (M= Co^{2+}, Cu^{2+}, L = a macrocyclic polyamine ligand) in basic aqueous solutions assisted by the concomitant transport of antiport halide ions[11]; b) the pH-gradient driven transport of amino acids by positively or negatively charged hydrophobic carriers;[12] c) the transport of hydrophobic amino acids from aqueous solution at the isoelectric point by Kemp's triacid-acridine 2:1 condensate;[13] d) the transport of phenylalanine in a neutral pH transport system

[a] Department of Chemistry, University of Michigan,
930 N. University Ave, Ann Arbor, MI 48109-1055, USA
Fax: (internat.) +1-734/647-4865
E-mail: dcouc@umich.edu

Supporting information for this article is available on the WWW under http://www.wiley-vch.de/home/eurjic or from the author.

  1434−1948/01/0303−0761 $ 17.50+.50/0

facilitated by cooperative ditopic interactions between the amino acid and unbound arylboronic acid and crown ethers;[14] e) the simultaneous transport of anions and cations by a neutral bifunctional receptor that contains calix[4] phosphate and an appended uranyl salophene unit;[15] f) the ditopic fixation and transport of amino acids with a bifunctional metalloporphyrin receptor;[16] g) the proposed ditopic transport of amino acids by lanthanide(III) tris(β-diketonate) complexes,[17] and; h) the use of phenylboronic acid/trioctylmethylammonium bromide as a carrier of amino acids through a dichloroethane BLM.[18] The enantioselective transport of amino acid derivatives also has been reported with chiral organic agents,[19] and several other metal complexes[20] have shown the ability to transport certain amino acids.

Our interest in supramolecules containing individual subunits with unique structural and reactivity properties[21] has led us to the synthesis of crown-functionalized salicylaldimine ligands. These compounds are readily obtained by Schiff-base coupling reactions between an appropriate salicylaldehyde and 1,2-diaminobenzo-crown ethers or 1,2,1′,2′-tetraaminodibenzo-crown ethers. The products that have been obtained thus far contain one tBu$_4$-salphen unit per 18-crown-6 unit (Figure 1A) and, more recently, 15-crown-5 and 12-crown-4 units.[22] With dibenzo-crown ethers, 2:1 tBu$_4$-salphen:crown ether molecules have been obtained with 18-crown-6 (Figure 1B), 24-crown-8, and 30-crown-10 units.[22b] The supramolecular coordination chemistry of crown ether-functionalized complexes[23] has been studied to a considerable extent and includes derivatives of salicylaldimines,[24] porphyrins,[25] and phthalocyanines.[26] The synthesis of derivatives of salphen ligands with 15-crown-5 ethers fused to the salicylidene rings has been reported.[27] The structures of these compounds[28] have not been determined, although their reactions with metal ions and elementary characterization have been reported.[29]

Metal complexes of the dinucleating ligands reported herein can be obtained readily by the incorporation of transition metal ions into the salicylaldimine portion of the ligand and, when available, alkali metal ions into the crown ether subunit. The presence of both electron pair accepting sites (the salicylaldimine-bound metal) and hydrogen bond accepting sites (the crown ether cavity) makes these molecules ideally suited for the recognition of zwitterions and amphiphilic molecules in general.

In previous communications,[30] we reported our studies on tryptophan and serotonin transport across a $CHCl_3$ BLM using crown ether-functionalized Mn^{III} and Ni^{II} complexes. In this paper we report in detail the synthesis and structures of these ditopic receptor molecules and our detailed studies of their use in the passive transport of tryptophan and serotonin across BLMs (Figure 2).

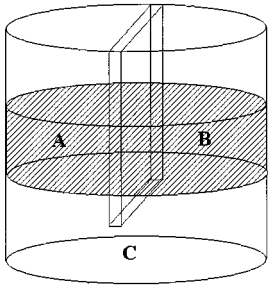

Figure 2. Bulk Liquid Membrane, BLM, transport cell: (A) and (B) source and receiving compartments; (C) $CHCl_3$ BLM

The active uptake of tryptophan is the first step in the synthesis of serotonin in the brain and is facilitated by a carrier that also transports other neutral and branched-chain amino acids. Serotonin is a very important neurotransmitter and influences a multitude of brain functions including sleep, cognition, sensory perception, motor activity, temperature regulation, appetite, sexual behavior, and hormone excretion.[31] Efficient synthetic carriers that facilitate the transport of both tryptophan and serotonin are not known.

Results and Discussion

Synthesis

The synthesis of *N*,*N*′-4,5-dimethoxybenzenebis(3,5-di-*tert*-butylsalicylideneimine) **(4)** and 4,5-bis(3,5-di-*tert*-butylsalicylideneimine)benzo-18-crown-6 **(9)** (Scheme 1) involves

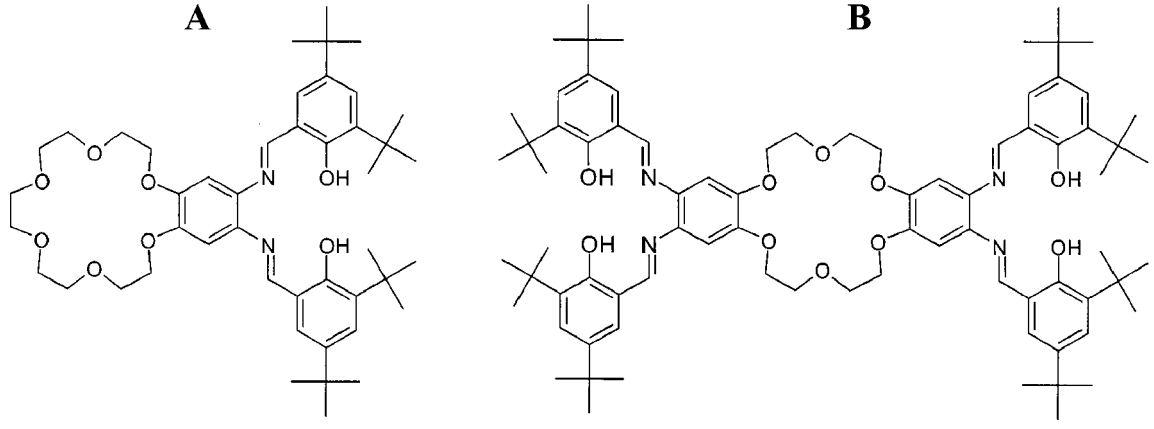

Figure 1. Ditopic Receptor Ligands: (A) tBu$_4$18-C-6; (B) (tBu$_4$)$_2$18-C-6

nitration of benzo-18-crown-6 followed by catalytic hydrogen reduction and Schiff-base condensation with the appropriate salicylaldehyde. The metal complexes of **4** (tBu$_4$M-Veratrole) and **9** (tBu$_4$M18-C-6) are obtained by addition of a methanolic solution of the metal salt to a chloroform solution of the ligand. Addition of "wet" methanolic solutions of alkali metal salts (KI, KCl, CsI, CsCl) to the chloroform solutions of the crown ether complexes allows for the introduction of alkali metal ions to the empty crown ether cavities. Complexes with two different Cs:M ratios were obtained by simply adjusting the CsI:M complex stoichiometry (M = Ni^{2+}, Mn^{3+}). An excess of salt usually yields the 1:1 (Cs^+ or K^+):tBu$_4$M18-C-6 complex.

The 1:2 (Cs^+):tBu$_4$M18-C-6 complexes are obtained when a 2:1 tBu$_4$M18-C-6:CsI ratio is used in the synthesis. The counterions that accompany the cationic Mn^{III} complexes can be exchanged readily with anions of the alkali metal salts. This often presents analytical problems and therefore the use of reagents with different anions is avoided.

Spectroscopic Characterization

The infrared spectra of the tBu$_4$M18-C-6 complexes in the region between 3500 cm^{-1} to 450 cm^{-1} are similar for different metal ions and dominated by the characteristic vibrations of the ligand. The spectra have been previously

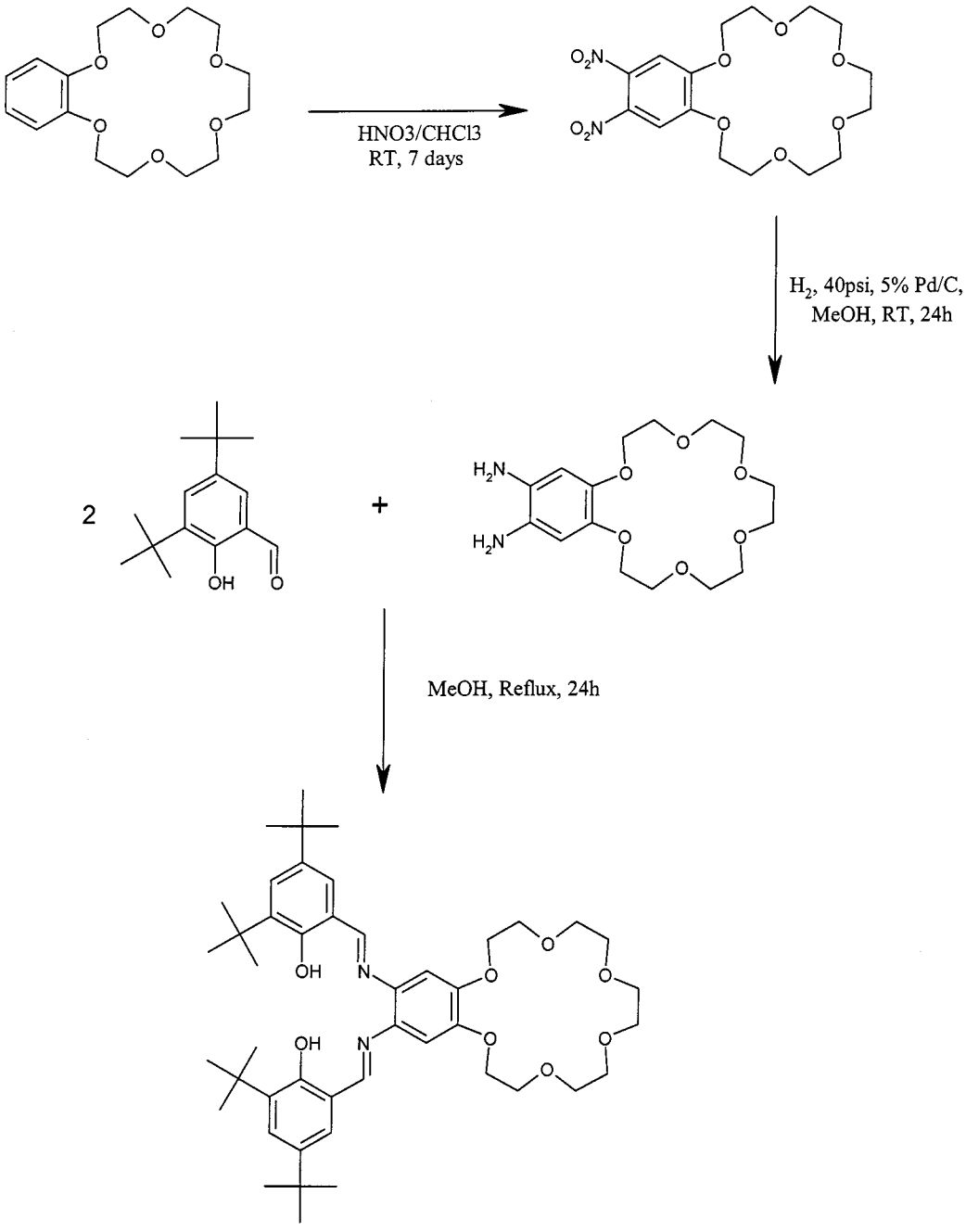

Scheme 1. Synthesis of tBu$_4$H$_2$18-C-6 **(9)**

assigned for the ligand as well as for the complexes. In the spectra of all the tBu$_4$M18-C-6 complexes the C=C stretching vibration occurs between 1595 and 1470 cm^{-1}, and the C=C out-of-plane bending at about 750 cm^{-1}. The C−H stretching of the *tert*-butyl groups is observed at 2960, 2910, and 2868 cm^{-1} and the imine stretch −C=N− is observed between 1620 and 1606 cm^{-1}. A C−O stretch for the phenolic oxygens of the salicylidene subunit is observed at about 1180 cm^{-1}. The out-of-plane C−H bending for the aromatic ring protons is observed at 820 to 846 cm^{-1}. The manganese complexes **5**, **6**, **15−28,** and **33** show the metal−oxygen stretch coupled with ring distortions around 540 cm^{-1}. Only very weak vibrations are observed in the far-IR region of the spectrum with features around 380 cm^{-1} and at times near 340 cm^{-1}.

Electronic Spectra

The electronic spectrum of ligand **9** shows two strong absorptions at 390 nm and 280 nm. The former is associated with an n−π* transition of the C=N group and the latter with a π−π* transition.[32] A shoulder at 239 nm is also due to a π−π* transition.[32] The spectra of the metal derivatives of **9** (tBu$_4$M18-C-6) (Table 1) are quite similar for different metal ions, even when alkali metal ions occasionally occupy the ether cavity. Generally, addition of transition metal ions to the salphen unit produces a change in color from the pale yellow color of the metal-free ligand to a deep red or brown color. In the Ni^{II} complex **10**, a sharp new band appears in the electronic spectrum at 496 nm, assigned to a charge-transfer transition from the ligand to the metal d orbitals (for Ni^{II}Salphen, the absorptions observed at 380−480 nm have previously been assigned[33] as charge transfer bands). The π−π* band at 266 nm in the free ligand also increases in intensity. Solutions of the Mn^{III} complexes **15−28,** and **33** in CH_2Cl_2 (Table 1) show broad bands at 490, 380, and 320 nm, and a sharper π−π* band at 260 nm [in the Mn(salen)X complexes, absorptions have been reported[34] at 588, 481, and 400 nm but only the visible region was scanned from 667−400 nm]. The electronic spectra of the tBu$_4$M18-C-6 complexes and the tBu$_4$MVeratrole complexes are similar.

Magnetic Susceptibility

The magnetic moments for the Mn^{III} complexes (Table 2) are all consistent with $S = 2$ ground states where variations from the spin only value (4.9 BM) may be due to spin-orbit coupling or inter/intramolecular interactions in the solid state. The complex **27**, with a structure similar to **14**, shows a magnetic moment (6.80 BM at 300 K and 6.26 BM at 4 K) less than that expected for two independent Mn^{III} centers (≈9.8 BM for 2 Mn^{III}) and indicative of antiferromagnetic coupling.

Table 2. Magnetics susceptibilities (μ_{eff}^{corr}/mol, in BM) for selected complexes at 300 and 4 K

	5[a]	**15**	**20**	**22**	**27**
300K	5.06	4.41	5.08	5.38	6.80
4K	4.88	4.38	4.84	4.95	6.26

[a] See Table 1 for the numbering scheme of complexes.

^{1}H NMR Spectroscopic Studies

The compounds, **3** and **9**,and their diamagnetic Ni^{II} derivatives, **4**, **10,** and **12−14**, could be characterized by ^{1}H NMR in a satisfactory manner in CD_2Cl_2 using the solvent as a reference. In the spectrum of **3**, the aromatic proton resonances appear at δ = 7.44, 7.28, and 6.87. The resonance for the imine proton is found at δ = 8.71 and for the *tert*-butyl protons at δ = 1.43 and 1.33. The Ni^{II} derivative **4** also shows a similar pattern with a large shift observable

Table 1. UV/Visible absorbances for the tBu$_4$M18-C-6 complexes **10−28** in CH_2Cl_2

	Abbreviated name	≈500	≈410	n-π* ≈390	≈350	≈310	π-π* ≈280	π-π* ≈260	π-π* ≈240
10	tBu$_4$Ni18-C-6	496	407	386	370		297	266	
11	tBu$_4$Ni18Cl· (HexNH$_3$Cl)	498	407	388	371		299	267	240
12	tBu$_4$Ni18-C-6(KI)	498	406	387	371		299	266	236
13	tBu$_4$Ni18-C-6(CsI)	496	406	387	372		296	266	
14	tBu$_4$Ni18-C-6(1/2 CsCl)	496	402	386	369	305	292	270	238
15	tBu$_4$Mn18-C-6Cl	483		380	364	319		263	
16	tBu$_4$Mn18-C-6I	493		379	356	321		262	
17	tBu$_4$Mn18-C-6(BPh$_4$)	471		377		320			
18	tBu$_4$Mn18-C-6(OAc)	485		375	358	318		260	
19	tBu$_4$Mn18-C-6(Piv)	489		374	355	316		262	
20	tBu$_4$Mn18-C-6Cl(KI)	500	419	384	354	326		259	
21	tBu$_4$Mn18-C-6Cl(KCl)	488		379	349	320		262	
22	tBu$_4$Mn18-C-6Cl(CsI)	498		381	356	320		262	
23	tBu$_4$Mn18-C-6Cl(CsCl)	488		376	353	319		262	
24	tBu$_4$Mn18-C-6Cl (1/2 CsCl)	487		379	348	321		262	
25	tBu$_4$Mn18-C-6I(KI)	495		379	349	314		261	
26	tBu$_4$Mn18-C-6I(CsI)	495		379	353	324		260	
27	tBu$_4$Mn18-C-6I (1/2 CsCl)	491		379	354	321		260	
28	tBu$_4$Mn18-C-6I(1/2 CsI)	495		377	348	322		260	

for the imine proton found at δ = 7.99. The remaining proton resonances are only slightly changed.

The ^{1}H NMR resonances of the salphen unit in **9** and its Ni^{II} derivative **10** are similar to those of their salen-veratrole counterparts. The assignment of the resonance peaks (Table 3) follow the numbering in Scheme 2. The protons of the phenol oxygen atoms in **9** readily exchange with water protons present in the solvent. The *tert*-butyl groups in all spectra are found at about δ = 1.3 to 1.4. The salphen unit of **9** shows the aromatic proton resonances at δ = 6.86, 7.22, and 7.44. These resonances, upon Ni^{II} coordination, shift to δ = 7.08, 7.13, and 7.38. The imine proton again shows the greatest shift upon metal complexation from δ = 8.66 to 7.96. The resonances due to the crown ether protons are unaffected by Ni^{II} coordination and are found at δ = 3.62, 3.66, 3.71, 3.90, and 4.23 in both **9** and **10**.

Table 3. ^{1}H NMR results of the *t*$Bu_4$18-C-6 compound **(9)** and its Ni^{II} complexes

	1[a]	2	3	4	5	6	7	8	9	10	11
9[b]	1.32	1.43	7.43	7.25	8.68	6.85	4.23	3.90	3.71	3.67	3.63
10[b]	1.32	1.44	7.39	7.16	8.04	7.14	4.23	3.90	3.72	3.66	3.62
10[c]	1.29	1.39	7.39	7.40	8.61	7.67	4.25	3.83	3.63	3.57	3.54
12[b]	1.32	1.44	7.39	7.16	8.03	7.14	4.23	3.90	3.72	3.67	3.62
12[c]	1.30	1.40	7.32	7.40	8.06	7.73	4.33	3.87	3.69	3.62	3.59
13[b]	1.35	1.47	7.44	7.74	8.61	7.43	4.41	3.57	3.49	3.55	3.57
13[c]	1.28	1.39	7.30	7.38	8.62	7.67	4.27	3.82	3.63	3.58	3.54
14[b]	1.35	1.48	7.45	7.81	8.78	7.35	4.42	3.83	3.62	3.52	3.43
	1.33	1.43	7.42	7.51	8.68	6.92	4.31		3.65	3.55	3.50
14[c]	1.29	1.40	7.32	7.40	8.63	7.68	4.27	3.83	3.65	3.59	3.55
10[d]	1.34	1.47	7.40	7.63	8.49	7.42	4.38	3.62	3.61	3.53	3.58
12[e]	1.32	1.45	7.39	7.16	8.04	7.15	4.24	3.90	3.72	3.67	3.64
13[e]	1.32	1.45	7.39	7.16	8.04	7.15	4.24	3.90	3.72	3.67	3.64

[a] See Table 1 for the numbering scheme of the complexes and Scheme 2 for the proton numbering scheme. − [b] Spectra taken in CD_2Cl_2. − [c] Spectra taken in D_6-DMSO. − [d] Spectrum taken in CD_2Cl_2 after the solution was saturated with a 0.100M CsI in D_2O solution. − [e] Spectrum taken in CD_2Cl_2 after the solution was saturated with D_2O.

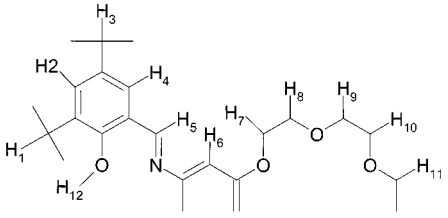

Scheme 2. Proton numbering for NMR spectra of the *t*Bu_4Ni18-C-6 complexes

When an alkali metal ion coordinates to the crown ether cavity, shifts can readily be seen in a non-coordinating solvent such as CD_2Cl_2. The alkali metal complexes show a remarkably different pattern in the crown ether proton resonances compared to those observed for **9** and **10.** Complexes **12**, **13**, and **14** show only three inequivalent sets of protons at around δ = 3.5, 3.6, and 4.3 with the resonance at δ = 3.6 accounting for twelve protons by integration of the areas. In the 1:2 Cs^+:complex **14** twice as many ^{1}H resonances are found as with the monomer **13**. This doubling of resonances reflects the loss of symmetry as a result of dimerization. The protons that point inside the pocket occupied by the Cs^+ ion are differentiated from the protons residing on the same carbon but oriented outside the pocket. This proton inequivalency shows that the "sandwich" complex (Figure 3D) that forms in the solid state stays intact in a noncoordinating environment.

In a coordinating solvent such as [D_6]DMSO, the spectra of the CsI derivatives **13** and **14** are identical and indicate dissociation of the alkali metal ions as a result of competition with the coordinating solvent. A common ^{1}H NMR pattern also is seen when CD_2Cl_2 solutions of the complexes **12**−**14** are saturated with D_2O. The resulting spectra are similar to that of **10**. An equilibrium between the complex **10** and CsI is evident when a saturated aqueous solution of CsI is extracted by a CD_2Cl_2 solution of **10**. The ^{1}H NMR spectrum of this solution of **10** exhibits resonance shifts that are similar to the 1:1 Cs^+:complex **13**. The same experiment with KI does not show any changes and perhaps reflects the insignificant partitioning of KI in CD_2Cl_2.

Description of Structures

[Nickel(II) 4,5-bis(3,5-di-*tert*-butylsalicylideneimine)benzo-18-crown-6] *n*-hexylammonium chloride (11)

The structure of **11** (Figure 3A) shows the benzo-18-crown-6 unit covalently attached to the Ni^{II}-*t*Bu_4Salphen unit. The Ni−O and Ni−N bond lengths (Table 4) are unexceptional and similar to those reported previously for other similar square planar complexes.[35] The *n*-hexylammonium cation that co-crystallizes with the ditopic receptor molecule in **11** shows the aliphatic chain oriented parallel to the *t*Bu_4Salphen unit at a distance of approximately 3.8 Å. The $-NH_3^+$ end is coordinated to the crown ether unit with the N atom nearly equidistant from the six ether oxygen donors. The average N−O distance of 2.92(4) Å is indicative of strong H-bonding interactions [N−O range 2.848(4)−3.032(4) Å]. This distance is slightly longer than the corresponding distance reported for the ammonium bromide "adduct" of 18-crown-6.[36] In **11** the nitrogen of the hexylammonium cation lies 0.901 Å above the plane formed by the crown ether oxygen atoms. The dihedral angle between the best plane defined by the six crown ether oxygen atoms and the NiO_2N_2 Ni^{II}-Salphen plane is 150°. This orientation places the Ni^{II} center approximately 8.5 Å from the crown ether O_6 centroid. In the lattice, pairs of individual **11** units are found nearly parallel to one another with the closest intermolecular Ni^{II}-18-crown-6 distance at 3.507 Å. The hexylammonium cations are located between the loosely held dimers and the Cl^- counterion is located 6.454 Å from the Ni^{II} ion.

[Nickel(II) 4,5-bis(3,5-di-*tert*-butylsalicylideneimine)benzo-18-crown-6]Cl (12-Cl)

In the structure of **12** (Figure 3B) the Ni^{II} coordination is also square planar and nearly identical to that found in **11** (Table 4). The Ni^{II} ion is located 0.0062(1) Å above the plane formed by the salicylidene oxygen and nitrogen donor atoms. A potassium cation resides in the crown ether pocket

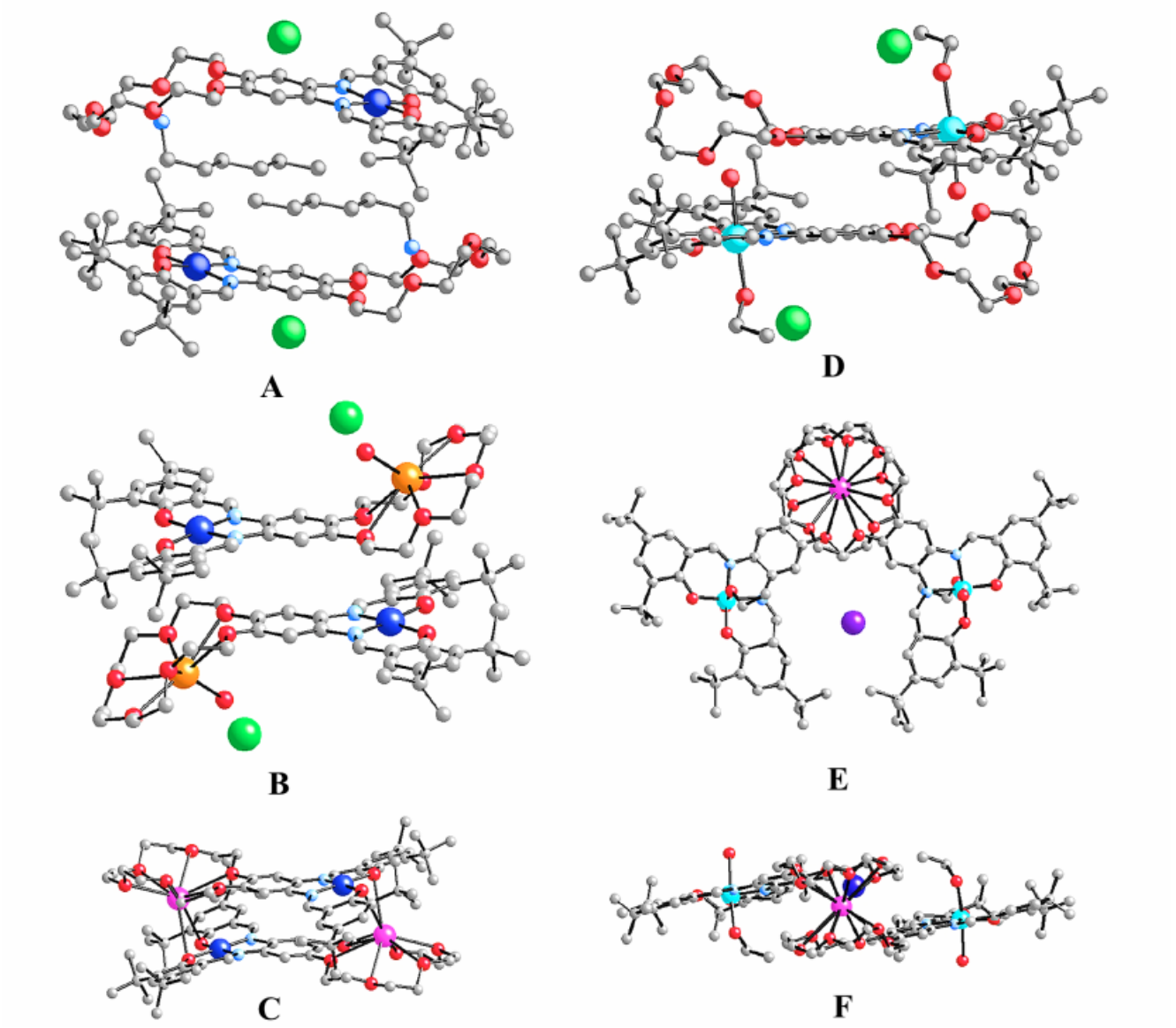

Figure 3. Molecular rendering obtained from Crystal Maker (color scheme: Ni blue; C grey; N light blue; O red; Mn aquamarine blue; K orange; Cs pink) using crystallographic coordinates of: (A) tBu$_4$Ni18-C-6[HexNH$_3$Cl] (**11**); (B) tBu$_4$Ni18-C-6(KI) (**12**); (C) the dimeric complex of tBu$_4$Ni18-C-6(CsI) complex (**13**); (D) tBu$_4$Mn18-C-6Cl (**15**), showing the hydrogen bonding between the H$_2$O ligand and the crown ether; (E) tBu$_4$uMn18-C-6I(1/2 CsI) (**28**); and (F) side view of the sandwich complex tBu$_4$Mn18-C-6I(1/2 CsI) (**28**)

Table 4. Selected bond lengths (in Å) for **11**−**15, 27**

	11[a]	**12**	**13**	**14**	**15**	**27**
M−O	1.843(6), 1.848(8)	1.866(2), 1.847(4)	1.864(4), 1.847(4)	1.90(2), 1.847(14)	1.866(2), 1.874(2)	1.84(2) 1.87(2)
M−N	1.859(2), 1.856(2)	1.868(2), 1.855(2)	1.849(4), 1.856(5)	1.90(2), 1.84(2)	1.992(3), 1.990(2)	1.96(2) 1.98(2)
M−L$_a$					2.214(3)	2.22(2)
M−L$_b$					2.289(3)	2.33(2)
C=N	1.303(3) 1.306(3)	1.307(3) 1.313(3)	1.284(8) 1.286(7)	1.30(3) 1.25(3)	1.302(4) 1.303(4)	1.33(3) 1.38(3)
C−O	1.301(2) 1.309(2)	1.310(3) 1.306(3)	1.331(7) 1.329(7)	1.28(2) 1.26(2)	1.323(3) 1.328(4)	1.43(3) 1.34(3)
C−O(ether)	1.42(3)	1.41(3)	1.42(4)	1.38(4)	1.41(3)	1.42(7)
A−O(ether)[b]		2.83(5)	3.05(9)	3.29(8)		3.34(12)

[a] See Table 1 for the numbering scheme of complexes. − [b] A represents the alkali metal coordinated to the cavity of the crown ether.

at a distance of 7.102(1) Å from the Ni^{II} ion. The K^+ ion is seven coordinate bound to the six oxygen atoms of the crown ether [avg. K−O = 2.83(2) Å; range 2.751(4)−2.899(4) Å] and a water molecule [$K-O_{H_2O}$ = 2.687(4) Å]. The potassium cation in **12** is located 0.747(4) Å above the best plane defined by the six crown ether oxygen atoms. The crown ether−K^+ bonding in **12** is similar to that reported for the potassium thiocyanate complex of 18-crown-6[37] (avg. K−O = 2.805 Å; range 2.770−2.833 Å). The chloride anion is found 3.478(1) Å from the K^+ ion, 7.102(1) Å from the Ni^{2+} ion and is hydrogen bonded to the K^+ bound water molecule at 3.409(3) Å. In the lattice, the closest Ni−Ni distance is 8.098(1) Å and the closest intermolecular contact is between Ni^{II} and O(8) at 3.507(3) Å.

[Nickel(II) 4,5-bis(3,5-di-*tert*-butylsalicylideneimine)benzo-18-crown-6]CsI (13)

In the structure of **13** (Figure 3C) the eight coordinate cesium ion is bound to the crown ether (Table 4) [avg. Cs−O = 3.08(3) Å; range 3.021(4)−3.177(4) Å] and two salicylidene oxygen atoms of another molecule at 3.298(4) Å and 3.266(4) Å. The dimeric arrangement is a consequence of the large ionic radius of Cs^+, which accommodates coordination numbers higher than six when associated with oxygen ligands. The coordination of the cesium in **13** is similar to that reported[38] for cesium thiocyanate with 18-crown-6 (avg. Cs−O = 3.146 Å; range 3.04−3.27 Å). Two nitrogen atoms (ordered thiocyanate anions) at 3.30 and 3.32 Å complete the eightfold coordination. The iodide anion for **13** is found 7.246 Å from the cesium ion and close to five carbon atoms at distances that range from 3.762(4) Å to 3.984(4) Å.

[Nickel(II) 4,5-bis(3,5-di-*tert*-butylsalicylideneimine)benzo-18-crown-6](1/2 CsI) (14)

In **14**, the cationic dimer (Figure 3D) contains two $C_{46}H_{64}N_2NiO_8$ units bound to a single cesium ion "sandwiched" between the two crown ether units. The cesium ion is twelve coordinate [avg. Cs−O = 3.30(3) Å; range 3.168(4)−3.445(4) Å]. In the structure, the two Cs^+-coordinated 18-crown-6 units are nearly parallel (dihedral angle between the two best O_6 planes is 3.1°) and staggered relative to each other. The distance of the cesium ion from the two planes is 1.832(4) Å and 1.741(4) Å. This arrangement is similar to a stack of 18-crown-6 units with cesium ions reported by Domasevitch, et al.[39] [avg. Cs−O = 3.265(8) Å; range 3.152(7)−3.431(8) Å]. In **14**, the iodide counterion is situated nearly equidistant from the two Ni^{2+} ions [6.867(2) Å and 6.952(2) Å] and the cesium ion [7.265(4) Å]. The Ni − Ni distance is 13.137(9) Å. Six solvent molecules are found in the lattice, a water molecule and five methanol molecules. All solvents are found at their sites at half occupancy.

Manganese(III) 4,5-bis(3,5-di-*tert*-butylsalicylideneimine)-benzo-18-crown-6-Cl (15)

In the structure of **15** the Mn^{III} ion occupies the tBu_4-Salphen unit and is octahedral, with the axial positions occupied by a water molecule [$Mn-O_{H_2O}$ = 2.289(3) Å] and an ethanol molecule ($Mn-O_{EtOH}$ = 2.214 Å). Both of these Mn−O bond lengths are in the range 2.21−2.29 Å so the ligands cannot be hydroxide or ethoxide (Figure 3E). The Mn^{III}−L distances, both axial and equatorial, are similar to that reported for the Mn(salen) acetate structure[40] [$Mn-O_{acetate}$ = 2.201(5) Å]. In **15**, the Mn^{III} ion is located 0.012(4) Å above the plane of the salicylidene oxygen and nitrogen atoms toward the ethanol ligand [in Mn(salen)-acetate[40] the Mn^{III} ion is found 0.017(4) Å out of the equatorial plane towards the acetate ligand]. Also found in the asymmetric unit were an additional ethanol molecule of solvation and the chloride anion [Mn−Cl = 4.541(1) Å]. The chloride anion is hydrogen bonded to the hydroxyl proton of the coordinated ethanol ligand [$Cl-O_{EtOH}$ = 3.085(4) Å] and the additional ethanol molecule of crystallization [$Cl-O_{EtOH}$ = 3.025(4) Å]. Short intermolecular hydrogen bonds in the crystal are observed between the Mn-bound H_2O ligand and the 18-crown-6 unit of another molecule. The dimeric arrangement (Figure 3E) again demonstrates the hydrogen bonding abilities of the crown ether units. The distance between the centroid of the crown ether and the manganese is 8.570(1) Å, and indicates that for effective direct crown ether-to-metal ditopic interactions the optimum donor-acceptor site separation within a zwitterionic guest should be around 8 ± 1 Å.

Bis[Manganese(III) 4,5-bis(3,5-di-*tert*-butylsalicylideneimine)benzo-18-crown-6 chloride]CsI (27)

The twelve coordinate Cs^+ cation in the dimeric **27** is located on a crystallographic twofold axis at 0, *y*, 1/4 in the space group *C*2/*c*. The general structure of the dimeric trication in **27** (Figure 3F) is very similar to that found in the structure of **14** (Table 4) and to a previously reported CsCl:benzo-18-crown-6 1:2 complex.[41] The iodide anion in the asymmetric unit is found in two positions with occupancies of 0.20 and 0.30 at 7.038(2) Å and 7.114(2) Å from the Mn^{III} ions and at 7.801(4) Å and 7.526(4) Å from the Cs^+ ion. The Mn−Mn distance at 13.113(9) Å is quite similar to the Ni−Ni distance in **14** of 13.137(9) Å. The chloride ion is also located at a position equidistant from the two Mn^{III} ions [8.14(1) Å]. In a manner similar to that described for **15**, each of the two Mn^{III} ions in **27** are axially coordinated by an ethanol and water molecules with M−O bond lengths of 2.33(2) Å and 2.22(2) Å, respectively.

Transport Properties of the Ditopic Receptors

The salphen-crown ether ditopic receptors are characterized by the availability of both an electron accepting site and an electron donating site within the same molecule. This availability allows the salphen-crown ether ditopic receptors to recognize and interact with amphiphilic guest

molecules. Important molecules of this type include amino acid zwitterions, or bifunctional molecules that contain acidic ammonium or basic carboxylate or hydroxo groups. The effective relative stability of 1:1 host-guest complexes is subject to size "matching" and is expected to be important in determining the selectivity features of host-guest interactions. The relative importance of a particular pair of interactions is difficult to evaluate when multiple interactive sites are present within the host and guest molecules. Generally, the sum of the $\Delta\Delta G$ values for the interactions involving host-guest complexation (following desolvation and/or reorganization events) will determine the thermodynamic feasibility of a given process.

In addition to the thermodynamic driving force required for transport ($\Delta\Delta G < 0$), favorable kinetics must allow for the association or dissociation of a guest molecule with a host carrier. An analysis of tryptophan and serotonin transport data obtained with various carriers leads to certain elementary conclusions and hypotheses regarding the transport properties of the salphen-crown ether ditopic receptors.

Tryptophan was chosen initially for transport experiments due to its hydrophobic nature relative to other amino acids and also its convenient electronic spectrum. It absorbs at 278 nm with an extinction coefficient of 5000 $M^{-1}cm^{-1}$, which permits sensitive detection in the millimolar range. In addition to the ammonium and carboxylate functional groups, tryptophan has additional sites for interaction, principally a phenyl ring that may $\pi-\pi$ stack with the aromatic rings of the salphen crown and the indole N−H group which may hydrogen bond to axial ligands on the metal center. The rate of tryptophan transport by numerous carriers was determined to evaluate the relative importance of the different sites. The benzo-18-crown-6 system was used as a benchmark against which all results could be compared. Transport studies with serotonin were carried out to determine the importance of size compatibility in the transport process.

An analysis of the fluxes[42] for the transport of tryptophan with various carriers (Table 5) shows a wide variation in the abilities of the salphen-crown ether hybrids to serve as carriers. The differences are associated mainly with the type of metal ion coordinated by the salphen ligand and also the type of alkali metal ion that may occupy the crown ether cavity. The role of the salphen-bound metal centers in the transport properties of the ditopic receptor carriers becomes apparent when the rate of tryptophan transport with the positively charged Mn^{III} complex **16** is compared to that of the free ligand **9**, the Ni^{II} complex **10**, the Cu^{II} complex **29**, and the corresponding $Fe^{III}-O-Fe^{III}$ dimeric complex[43] (Figure 4). In **9**, **10**, and **29**, the carrier is neutral and is not subject to significant electrostatic interactions with the tryptophan zwitterion. Furthermore, the ligand field stabilizations of the square Ni^{II} and Cu^{II} centers in **10** and **29** preclude any strong axial interactions with the carboxylate functional group on the amino acid. As a result, **9, 10,** and **29** are inferior carriers relative to **16** and their transport properties are similar to those exhibited by simple crown ethers. The transport of tryptophan by the neutral $Fe^{III}-O-Fe^{III}$ complex, however, is significant and proceeds at approximately 70% the rate observed for the Mn^{III} cation. In **16,** the best carrier in the group, the Mn^{III} ion not only carries a net positive charge but also has a propensity to bind axially coordinated ligands. The superior transporting character of **16** relative to the $Fe^{III}-O-Fe^{III}$ dimer may be due to the electrostatic interactions, which are significant for the former but weak or absent for the latter.

Table 5. Calculated fluxes of the selected complexes (based on 24 h measurement)

Cmpd	Abbrv. Name	Flux[a]	Cmpd	Flux[a]	Cmpd	Flux[a]
Bz18-C-6		2.36	**13**[b]	1.52	**21**[b]	4.94
4	tBu$_4$NiVeratrole	0	**14**[b]	1.52	**22**[b]	40.5
	(tBu$_4$Fe18-C-6)$_2$O	40.2	**15**[b]	32.5	**23**[b]	6.67
5	tBu$_4$MnVeratrole Cl	6.92	**16**[b]	54.9	**24**[b]	6.14
6	tBu$_4$MnVeratrole I	1.12	**17**[b]	109	**25**[b]	20.8
9	tBu$_4$H$_2$18-C-6	2.04	**18**[b]	9.92	**26**[b]	41.5
10[b]		1.48	**19**[b]	62.5	**27**[b]	36.2
12[b]		0.48	**20**[b]	8.70	**28**[b]	29.2

[a] The unit for flux is (mol/second/mol Carrier/m^2) $\times 10^{-4}$ – [b] The abbreviated name for this compound can be found in Table 1.

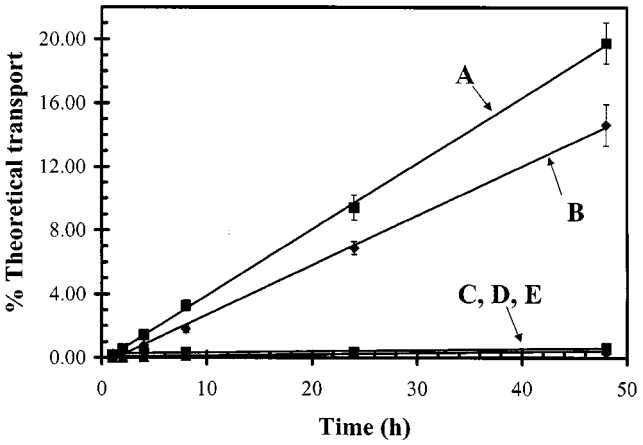

Figure 4. $CHCl_3$ BLM transport of tryptophan by 0.9 mM solutions of the carriers: (A) tBu$_4$Mn18-C-6I **(16)**; (B) [tBu$_4$Fe18-C-6]O, Fe−O−Fe dimer; (C) tBu$_4$Ni18-C-6 **(10)**; (D) tBu$_4$Cu18-C-6 **(29)**; (E) tBu$_4$H$_2$18-C-6 **(9)**; the initial concentration of tryptophan in the source phase was 50 mM

The initial transport rates of tryptophan and serotonin by tBu$_4$Mn18-C-6X (X = I, Cl) were determined as a function of carrier concentration (Figure 5) and showed first order dependence. In this concentration-gradient driven process, the concentrations of tryptophan or serotonin in the source and receiving compartments of the transport cell eventually become equal as the system asymptotically approaches equilibrium. First order rate constants obtained from these plots by linear fits of the data (Figure 5) show a slower rate of transport for serotonin (Figure 5C) than for tryptophan (Figure 5A).

For the facilitated transport of a given solute through a membrane by a membrane-residing carrier, C_m, the flux, J_{solute}, is defined as[44]:

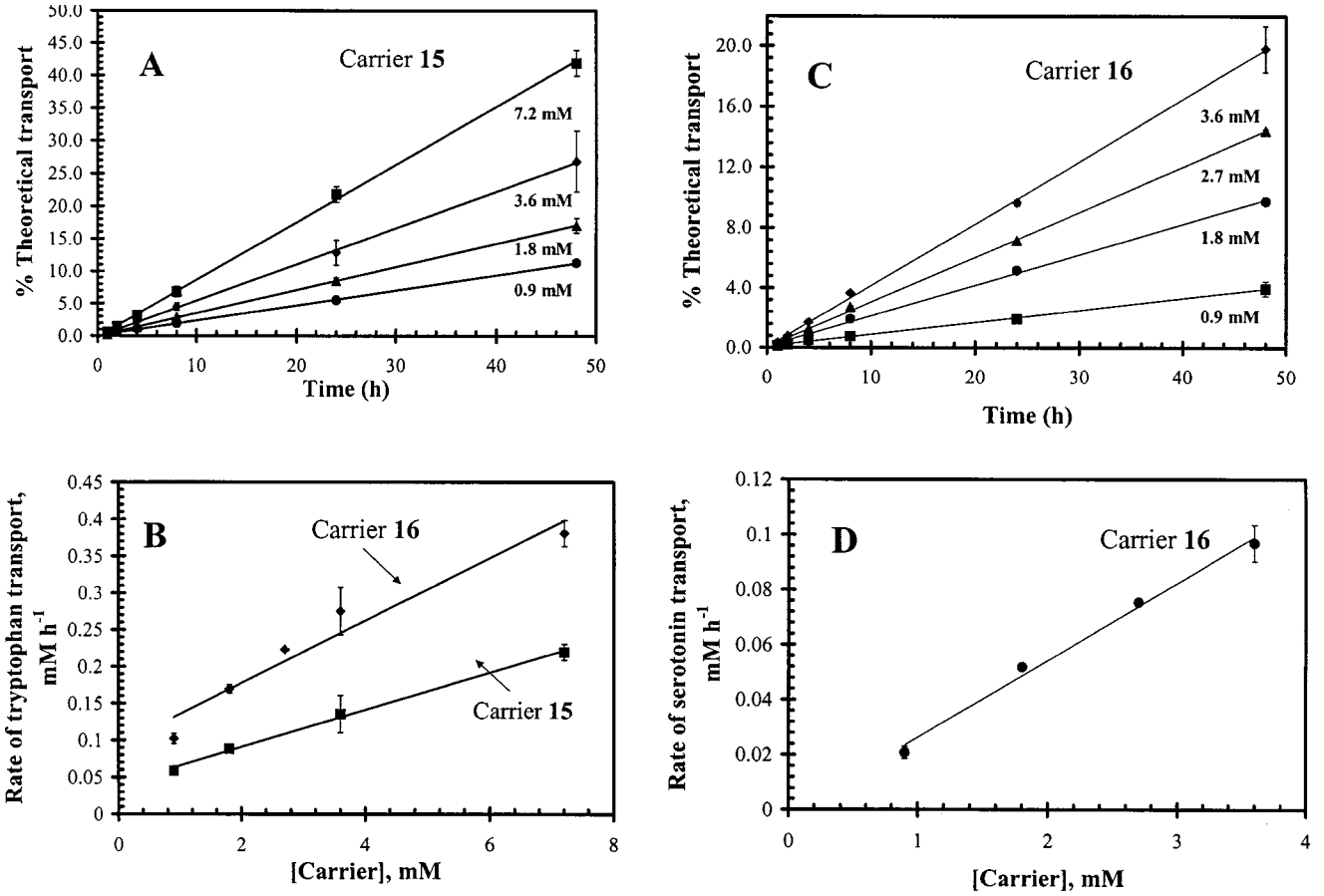

Figure 5. (A) $CHCl_3$ BLM transport of tryptophan as a function of tBu$_4$Mn18-C-6Cl **(15)** carrier concentration; the concentration of carrier varied from 0.9−7.2 mM; (B) plots of the rate of tryptophan transport vs. carrier concentration for tBu$_4$Mn18-C-6I **(16)** and tBu$_4$Mn18-C-6Cl **(15)**; (C) $CHCl_3$ BLM transport of serotonin as a function of tBu$_4$Mn18-C-6I **(16)** carrier concentration; the concentration of carrier varied from 0.9−7.2 mM; (D) plot of the rate of serotonin transport vs. concentration of tBu$_4$Mn18-C-6I; the initial concentration of tryptophan in the source phase was 50 mM

$$J_{solute} = \frac{D_{cs}C_oK_{ex}}{L}\frac{S_s - S_r}{(1+K_{ex}S_s)(1+K_{ex}S_r)}$$

where D_{cs} = carrier−solute diffusion constant, C_0 = total concentration of carrier, S_s = concentration of solute at source interface, S_r = concentration of solute at receiving interface, L = membrane thickness, and $K_{ex} = [CS_m]/[S_s][C_m]$. When K_{ex} is not very small and/or S_s is reasonably large (such as early in the transport process), then $K_{ex}S_r << 1$ and the flux is given by:

$$J_{solute} = \frac{D_{cs}C_oK_{ex}S_s}{L}\frac{S_s}{(1+K_{ex}S_s)}$$

which is of the form of the Michaelis−Menten equation for the process:

$$C_m + S_s \xleftrightarrow{Kex} [CS_m] \rightarrow C_m + S_r$$

The Michaelis−Menten constant K_m ($K_m = [S_s][C_m]/[CS_m] = 1/K_{ex}$) can be obtained from double-reciprocal Lineweaver−Burk plots. The transport of tryptophan and serotonin were followed as a function of substrate concentration and found to follow Michaelis−Menten kinetics. From Lineweaver−Burk plots (Figure 6), K_m values of 25 mM and 245 mM were determined for tryptophan and serotonin transport, respectively. From these apparent Michaelis constants carrier-permeant extraction constants ($K_{ex} = 1/K_m$) of 40 M^{-1} and 4 M^{-1} were determined for the tryptophan and serotonin carrier complexes, respectively. The origin of this difference in K_m and K_{ex} values is difficult to ascertain considering the multitude of interactions that contribute to various extents to the overall free energy of carrier-guest complexation. Practical difficulties in maintaining control of pH and their effects in the transport process also make comparisons difficult. Phenomenologically, one may expect weaker Mn−O bonding with the protonated phenolic oxygen donor of serotonin than with the carboxylate group of tryptophan. In such a case, and considering other events energetically similar, one may attribute the differences to differences in Mn−O interactions.

Kinetic studies as a function of temperature for tryptophan and serotonin transport and Arrhenius plots (Figure 7) yielded activation parameters (Table 6). The energies of activation E_a of 20 ± 1 and 17 ± 5 kJ mol^{-1} indicate diffusion-controlled processes.[44]

Studies were conducted to determine the relative transport efficiency of the ditopic receptors by comparison to

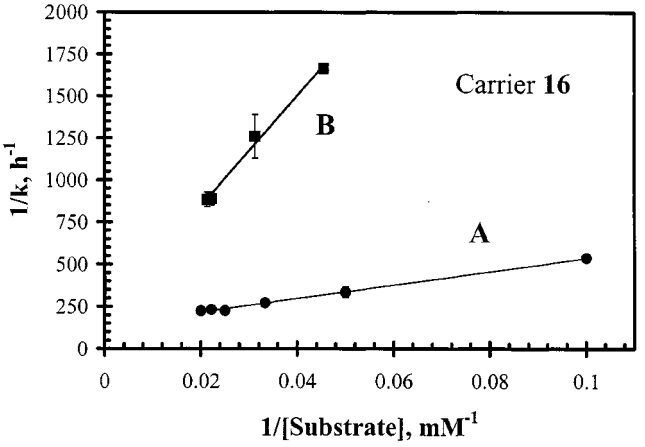

Figure 6. Lineweaver−Burk plots for: (A) tryptophan transport, and (B) serotonin transport with *t*Bu$_4$Mn18-C-6I **(16)** as the carrier; concentrations of tryptophan and serotonin were 10−50 mM and 22−47 mM, respectively

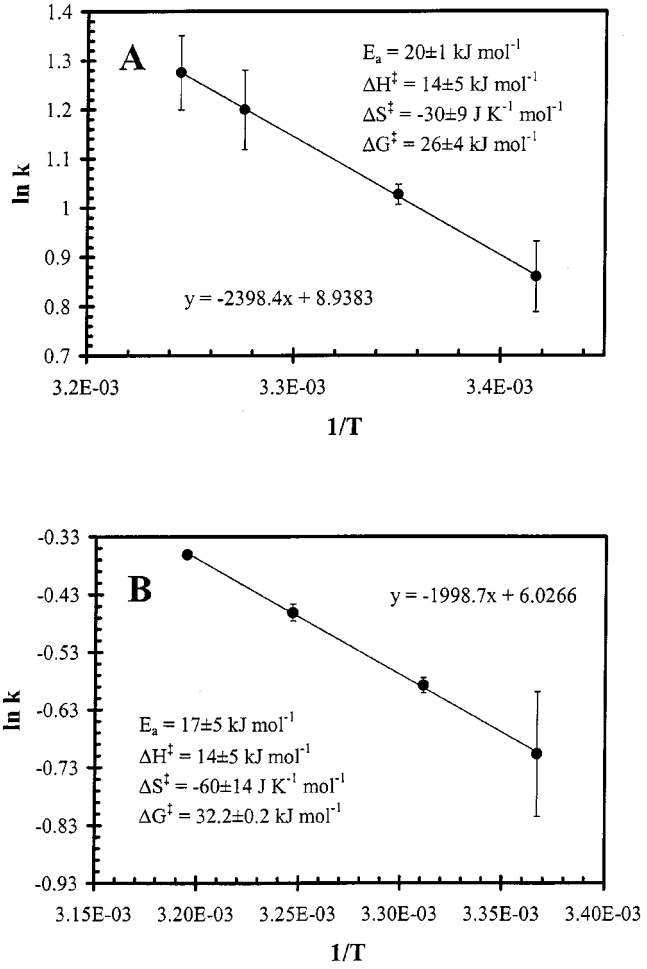

Figure 7. Arrhenius plots for: (A) tryptophan, and (B) serotonin transport with *t*Bu$_4$Mn18-C-6I **(16)** as the carrier; temperature range: 297−315 K

that of an equimolar mixture of two closely related monotopic half-receptors. The transport of tryptophan by a 1:1 mixture of Mn^{III} *N*,*N*′-dimethoxybenzenebis(3,5-di-*tert*-butylsalicylideneimine) iodide **(6)** and benzo-18-crown-6 were compared to those of **16** and also of **6** and benzo-18-crown-6 individually. The results show (Figure 8A) that in an equimolar mixture the two carrier components of **16** function synergistically. The rate of transport observed with **16**, however, is still 30% faster and indicative of moderate ditopic cooperativity. The same experiments carried out with serotonin (Figure 8B) show greater ditopic cooperativity and can be attributed to a better spatial matching between the donor-acceptor pairs within the serotonin-**16** complex. The synergism displayed by the mixture of the two carrier components of **16** in the transport of tryptophan and serotonin (Figure 8) has been reported previously for equimolar mixtures of arylboronic acids and crown ethers in the transport of L-phenylalanine through $CHCl_3$. Similarly, the ditopic cooperativity shown by **16** in the transport of tryptophan, which is more pronounced in the transport of serotonin, has been reported previously for crown ether-functionalized boronic acids in the facilitated transport of catecholamines.[45] The synergism observed in the tryptophan transport by a 1:1 mixture of benzo-18-crown-6 and **6** suggests that the transport of tryptophan by **16** may proceed simultaneously by first and second order reactions. A plot of the tryptophan transport rate as a function of carrier concentration (Figure 5) and an attempted fit with a second degree polynomial did not show evidence for a second order process, where two molecules of **16** act in tandem in the transport process.

The Role of the Crown Ether Unit

The salphen-crown ether ditopic receptors are capable of lowering the kinetic barrier associated with the $H_2O-CHCl_3$ interface transport of the carrier-guest complex. This is due to the ability of the relatively hydrophilic crown ether to "invade" the water solution across the interface. The covalently bound highly hydrophobic salphen unit precludes the partitioning of the carrier into the water. The importance of the crown ether in the transport of tryptophan is apparent when **16** is compared to the *t*Bu$_4$MnVeratrole complex **6** (Figure 9). The latter is a complex similar in most aspects to **16** except that it lacks the crown ether appendage. The electronic structural similarities[46] between **6** and **16** notwithstanding, the rates of tryptophan transport between **6** and **16** differ significantly and indicate that the crown ether unit plays an important role in transport. This undoubtedly derives from the hydrogen-bond-accepting nature of the crown ether cavity and its ability to interact with $-NH_3^+$ groups. This type of interaction has been previously established in various structure determinations[47] and also in the structure of **11** (Figure 3A).

The importance of an unhindered crown ether group in the transport of tryptophan is further demonstrated in the difference in transport rates between the salphen-crown, such as **16**, and the salphen-crown-salphen carriers, such as **33** (Figure 1B). The former shows transport rates (Figure 9) far superior to those observed with the latter with two metal-salphen units. A reason for this counter-intuitive difference may be the additional hydrophobic unit in **33** that effectively blocks the crown ether from penetrating across the interface. Nevertheless, the possibility that this differ-

Table 6. Michaelis–Menten K_m and V_m values and activation parameters for the rate of transport of tryptophan and serotonin

Substrate	K_m(mM)	V_m(h^{-1})	E_a(kJ mol^{-1})	$\Delta H^{\ddagger}$(kJ mol^{-1})	$\Delta S^{\ddagger}$(J mol^{-1})	$\Delta G^{\ddagger}$(kJ mol^{-1})
Tryptophan	25.4	0.00675	20±1	17±1	−30±9	26±4
Serotonin	245	0.00712	17±5	14±5	−60±14	32±1

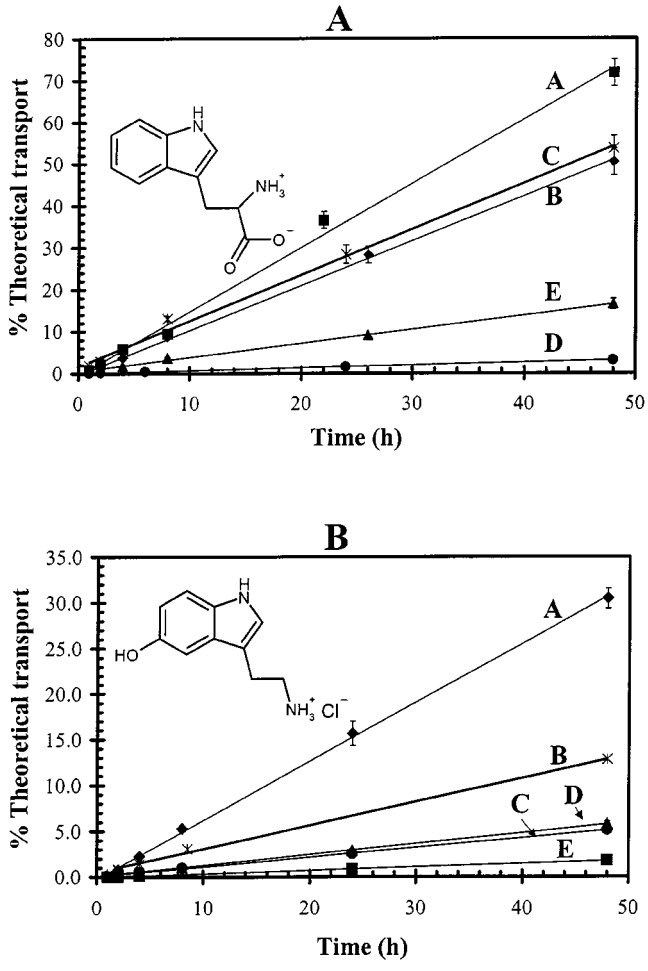

Figure 8. **A:** $CHCl_3$ BLM transport of tryptophan by 7.2 mM solutions of: (A), tBu$_4$Mn18-C-6I; (B), benzo-18-crown-6 + tBu$_4$MnVeratroleI (1:1 molar ratio); (C), tBu$_4$Mn18-C-6I + KI (1:1 molar ratio); (D), tBu$_4$MnVeratroleI; (E), benzo-18-crown-6. The initial concentration of tryptophan in the source phase was 50 mM; **B:** $CHCl_3$ BLM transport of serotonin by 7.2 mM solutions of: (A), tBu$_4$Mn18-C-6I; (B), tBu$_4$Mn18-C-6I + KI (1:1 molar ratio); (C), tBu$_4$MnVeratroleI; (D), benzo-18-crown-6 + tBu$_4$MnVeratroleI (1:1 molar ratio); (E), benzo-18-crown-6

ence still may be partly due to the differences in donor properties between the benzo-18-crown-6 and dibenzo-18-crown-6 units should not be overlooked. In the dibenzo-18-crown-6 units, weaker donor properties may be displayed due to the presence of only two aliphatic ether oxygen donors.[48]

An examination of the transport properties of the tBu$_4$Mn18-C-6X (**15** and **16**) and tBu$_4$MnVeratroleX (**5** and **6**) carriers (X = Cl and I; Figure 10) shows the I^- salt of the former to be better than the Cl^- salt. The opposite is observed with the latter, where **5** shows a faster transport rate than the corresponding I^- salt, **6**. The crown ether unit

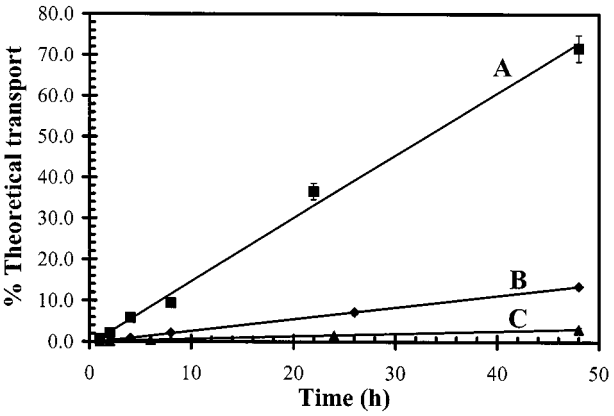

Figure 9. $CHCl_3$ BLM transport of tryptophan by 7.2 mM solutions of: (A) tBu$_4$Mn18-C-6I, (B) (tBu$_4$Mn)$_2$18-C-6I, and (C) tBu$_4$MnVeratroleI; the initial concentration of tryptophan in the source phase was 50 mM

common to **15** and **16** allows the penetration of these carriers across the interface and the higher transport rate of the I^- carrier **16** is very likely due to its higher ionic nature relative to the Cl^- analog, **15** (vide infra). In **5** and **6**, the absence of the crown ether appendix underscores the need for a different kinetic factor for facilitating interface crossing. A possible explanation for the halide effects in the transport properties of **5** and **6** is that the less hydrophobic Cl^- salt is more likely to effectively approach the interface than the I^- salt. It appears that, in transport with the tBu$_4$MnVeratroleX carriers, the ability to approach the interface becomes the rate-determining step.

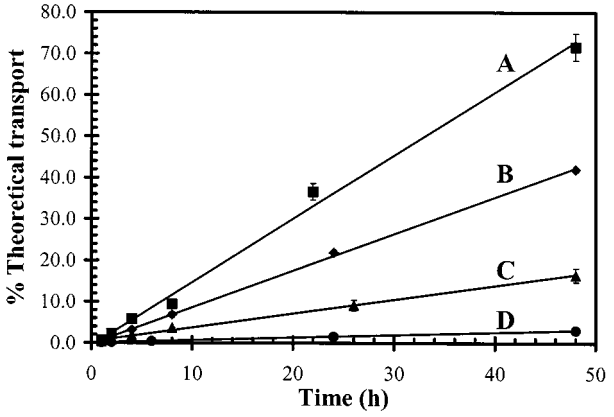

Figure 10. $CHCl_3$ BLM transport of tryptophan by 7.2 mM solutions o: (A) tBu$_4$Mn18-C-6I, (B) tBu$_4$Mn18-C-6Cl, (C) tBu$_4$MnVeratroleCl, and (D) tBu$_4$MnVeratroleI; the initial concentration of tryptophan in the source phase was 50 mM

The Effects of Alkali Metal Ions

The beneficial contributions of the crown ether units in the transport of tryptophan are diminished when alkali metal ions are introduced to the crown ether cavities of **15**

and **16**. Alkali metal ions are well-known to bind strongly to crown ethers in interactions that depend greatly on size matching between the ionic radius of the cation and the crown ether cavity.[49] The effects on the rate of tryptophan transport when alkali metal ions are competing with the $-NH_3^+$ moiety of the amino acid are as expected, and show a decrease in the rate of tryptophan transport when K^+ or CsCl salts are present at various concentrations. With CsI, the rate of transport depends on the concentration of Cs^+ in the $CHCl_3$ phase. With both **26** and **28**, the rate of transport slightly increases relative to that in the absence of the Cs^+ ion. Once a saturated aqueous solution of CsI is used in both the source and receiving compartments, the rate decreases following the behavior of the other alkali metal salts. The alkali metal salt-effect has been studied in the transport of amino acids into cells of *Streptomyces hydrogenans*, where K^+ or Rb^+ salts were introduced into a solution of the amino acid and an increase in the transport rate into the cell was observed.[50] In the present systems, the aqueous source and receiving compartments in transport experiments using carriers **20**−**28** were analyzed for the appropriate alkali metal salt by both conductivity experiments and HPLC analyses. These analyses showed that at least 95% of all K^+ salts and CsCl leached into the aqueous solutions after the first hour of transport. These results support the contention that the alkali metal-induced decrease in the tryptophan transport rate is due to the competition of the alkali metal cations with the $-NH_3^+$ group of tryptophan for the crown ether "tail" of the carrier as it penetrates the interphase. This is not the case with the CsI "adducts" **26** and **28**. The concentration of CsI in the aqueous phases in contact with $CHCl_3$ solutions of **26** and **28** tended to be consistently lower and, at equilibrium, only 75% of the total amount of CsI had leached out. The hydrophobicity of the CsI and its association with the carriers **26** and **28** in $CHCl_3$ solution may be the reason for the transport-rate enhancement found with the complexes **26** and **28**. However, the specific host-guest interactions involved in tryptophan transport with **26** and **28** are not clear and may have their origin in the unique structure of **28**, which persists in $CHCl_3$ solution. The ^1H NMR spectrum of the Ni^{II} complex **10** in CD_2Cl_2 (saturated with CsI) exhibits resonances reminiscent of the spectrum of tBu$_4$Ni18-C-6(CsI) **(13)**. This behavior demonstrates a significant tendency of CsI to partition into the organic phase and interact with the carrier.

Axial Interactions with the Mn^{III} Center

Numerous positively charged Mn^{III} salen complexes are known with the counterions bound to the metal (in noncoordinating solvents), forming square pyramidal complexes.[51] In coordinating solvents, the cationic Mn^{III} complexes form 2:1 solvent adducts with an octahedral geometry. This is also demonstrated in the crystal structures of **15,** which show that when **15** is crystallized from a methanol solution, the metal accepts two axially coordinated solvent molecules, whereas crystallization from ethyl acetate gives a derivative with the chloride counterion coordinated to one of the two axial sites on the metal.[52] The electronic spectra of the complexes **15**−**19** in CH_2Cl_2 solution are all unique and show varying magnitudes of axial ligand−metal ion interactions, as evidenced by the location of an electronic absorption band between 470 and 500 nm (Table 1). The tetraphenylborate salt **17** shows this absorption at the shortest wavelength (470 nm). Taking into account the noncoordinating properties of this anion, the absorbance is probably due to coordination of the MeOH present in the CH_2Cl_2. Indeed, a common band is observed at 460 nm for all complexe **15**−**19**, in MeOH solution (Table 7). The bathochromic shifts of the 470 nm band, caused by coordination of electron donors to the Mn^{III} center in **15**−**19**, indicate that this electronic absorption is very likely due to a metal-to-ligand charge transfer (MLCT) process. The relative substrate transport rates are slower for carriers that show the larger bathochromic shifts of the MLCT band (Table 1). The differences in the bathochromic shift of the CT absorption reflect differences in strength of the Mn^{III}-axial ligand interactions. Generally, the transport data indicate that the less coordinating anions do not compete effectively with the amino acids for the Mn^{III} site. As a result, the efficiency of tryptophan transport follows the order: $B(Ph)_4^- > I^- = Piv^- > Cl^- > Ac^-$ (Figure 11). This is also the order by which Λ_m, the molar conductivity, increases (Table 7). The conductance measurements indicate that hydrophobic $CHCl_3$−ion interactions promote ionic dissociation in $CHCl_3$ solution.

As a consequence, the greater donor properties of the pivalate anion, with an expected superior solubility in nonaqueous media and anticipated stronger interactions with the Mn^{III} center, are not reflected in the transport rate of tryptophan by it; the latter shows a higher transport rate than the acetate salt **18**.

With tetraphenylborate as a counterion for the Mn^{III} carrier, compound **17** shows a considerable increase in the rate of tryptophan transport. This is noteworthy considering the limited solubility of **17** in $CHCl_3$. Indeed, the solubility of **17** is considerably less than that of the other carriers. The origin of this reduced solubility of **17** in nonaqueous media may be due to extensive charge localization in the carrier ion-pair. The bulky tetraphenylborate anion, which is unable to coordinate to the metal ion, leaves a full positive charge on the metal. Similar arguments may be made for the iodide salt **16**, which also shows fast transport rates. In addition to hydrophobicity, another reason for the increase in the rate of transport observed with the tetraphenylborate and iodide salts may be that these weakly interacting anions allow the salphen-bound metal to interact with the aqueous phase and coordinate axial H_2O ligands (vide infra).

Host−Guest Interactions

In the zwitterionic form, amino acids can interact either with the RNH_3^+ group (with the crown ether site in the carrier) or with the $R-COO^-$ group (with the Mn^{III} site). With hosts such as **16**, the host-guest interactions cannot be ditopic due to the short span of the amino acid functional groups relative to the separation between the Mn^{III}

Table 7. Comparison of the electronic spectra and molar conductivity between carrier complexes with different anions in CH_2Cl_2 and MeOH

Complex	λ_{max} of the MLCT band in CH_2Cl_2 (in nm)	λ_{max} of the MLCT band in MeOH (in nm)	Λ_m ($\mu S\ cm^2\ mol^{-1}$)
15[a]	483	460	4
16	498	460	15
17	471	460	325
18	485	460	3
19	489	460	15

[a] The abbreviated name of this compound can be found in Table 1.

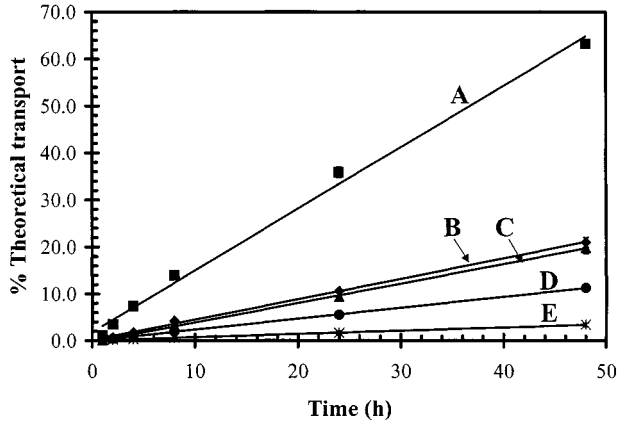

Figure 11. Effect of the anion, X, in the transport of tryptophan by 0.9 mM solutions of the tBu$_4$Mn18-C-6X carriers: (A) tBu$_4$Mn18-C-6(BPh$_4$) **(17)**, (B) tBu$_4$Mn18-C-6(Piv) **(19)**, (C) tBu$_4$Mn18-C-6I **(16)**, (D) tBu$_4$Mn18-C-6Cl **(15)**, and (E) tBu$_4$Mn18-C-6(OAc) **(18)**; the initial concentration of tryptophan in the source phase was 50 mM

center and the crown ether cavity. This distance becomes shorter when H_2O is added axially to the Mn^{III} center and should make it possible for the zwitterionic amino acid guest to hydrogen-bond to the water molecules through the carboxylate group and simultaneously to the crown ether cavity through the ammonium group. The observed ditopic behavior (Figure 8) very likely reflects transport with a water-coordinated Mn^{III} center. Molecular mechanics calculations[53] on the tryptophan-tBu$_4$Mn18-C-6 complex support this suggestion and show (see Figure 12) that, when tryptophan is placed in the pocket of the carrier that contains a water molecule axially coordinated to the Mn^{III} center, the relative energy of the host-guest complex decreases.[53] In the energy-minimized structure, in addition to RNH_3^+ hydrogen bonding with the crown ether appendix ($RNH_3^+\cdots O$, 2.69 Å), short hydrogen bonds are found between the amino acid carboxylate group and the Mn^{III}-bound water molecule($COO^-\cdots H_2O-Mn$, 2.51 Å). In the energy-minimized structure without the Mn^{III}-bound water molecule, the only hydrogen bonding interaction is between the RNH_3^+ unit and the crown ether unit ($RNH_3^+\cdots O$, 2.69 Å; $COO^-\cdots Mn$, 3.79 Å). The same type of calculations was performed with serotonin. With a water molecule axially bound to the Mn^{III} ion in **16** the energy minimized structures (Figure 13) show the relative energy of the serotonin-**16** complex[53] much higher than that of the complex without an axially bound water molecule. The lower energy of the latter is not unexpected considering the favorable spatial disposition of the donor (OH group) and acceptor (NH_3^+ group) sites in the serotonin molecule at a distance of 8.35 Å. This distance is comparable to the Mn^{III}-crown ether centroid distance of 8.72 Å and allows for an optimal host-guest interaction. This interaction accounts for the superior ditopic effect shown in the serotonin transport by **16** (Figure 8B) relative to the transport of tryptophan by the same carrier (Figure 8A).

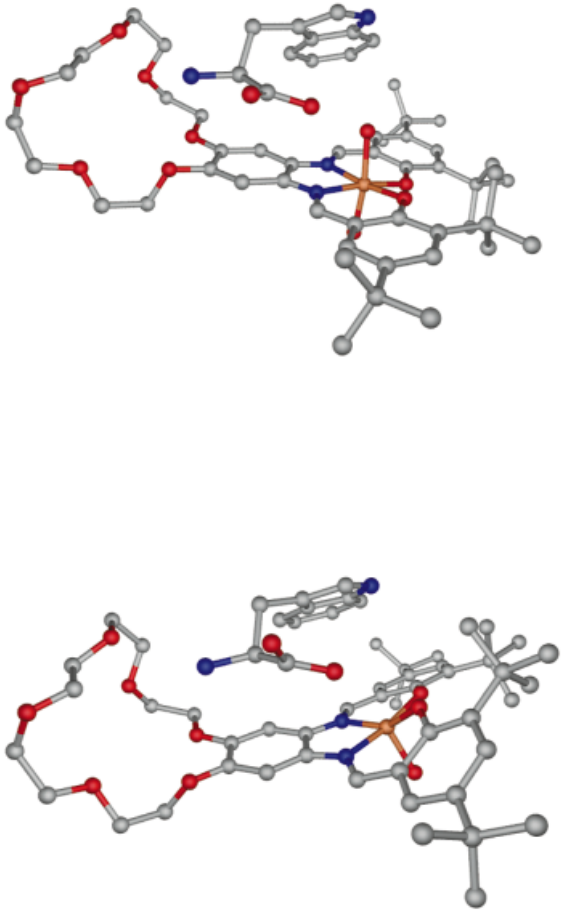

Figure 12. Optimized structures of the tryptophan-tBu$_4$Mn18-C-6 complex: (A) with, and (B) without an Mn-coordinated H_2O ligand

Other modes of interaction are possible with tryptophan and the ditopic carriers. These include a contact between

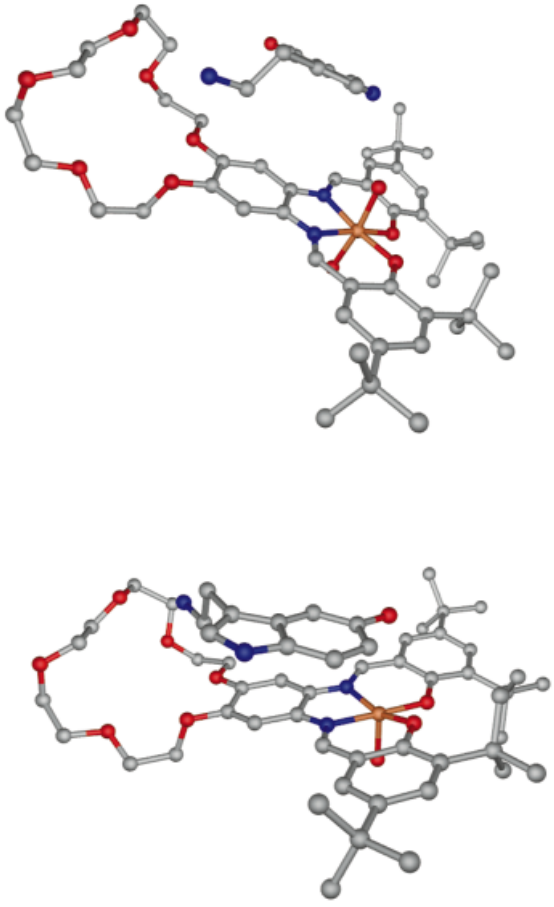

Figure 13. Optimized structure of the serotonin-tBu$_4$Mn18-C-6 complex: (A) with, and (B) without an Mn-coordinated H_2O ligand

the aromatic ring of tryptophan and the "bridging" aromatic ring of the carrier through π-stacking and also simple hydrophobic interactions of tryptophan with the organic phase. The use of leucine and phenylalanine in transport experiments was undertaken to explore the possible importance of these modes of interaction. Solubility data indicate that both are slightly less hydrophobic than tryptophan (11.4 mg TRP/mL H_2O at 23 °C, 24.3 mg LEU/mL H_2O at 25 °C, and 29.7 mg PHE/mL H_2O at 23 °C[54]). The rates of transport of the three amino acids show a dependence on hydrophobicity but not on aromaticity and suggest that the rates depend on the ability of the amino acids to approach and enter the organic solvent-water interface.

Conclusion

A new class of ditopic receptor molecules has been synthesized and structurally characterized. The unique structural features of these molecules are: a) a very lipophilic unit that consists of two 3,5-di-*tert*-butylsalicylideneimine moieties that form a square O_2N_2 coordination site, and b) a relatively hydrophilic benzo-18-crown-6 ether unit capable of binding to alkali metal ions and hydrogen bonding with ammonium functional groups. These molecules, which are totally insoluble in water but very soluble in nonpolar solvents, have been found to be effective in the facilitated transport of hydrophobic amino acids and serotonin across $CHCl_3$ bulk liquid membranes.

The metal ion within the O_2N_2 coordination site, and its affinity for axial ligands, determines transport efficiency. The neutral Ni^{II} derivatives of the ditopic receptors, with little affinity for axial ligands, are poor carriers and their efficiency in the transport of tryptophan is roughly equal to the unmetallated ligands or benzo-18-crown-6 ether. In contrast, the monocationic Mn^{III} derivatives are very efficient carriers in the facilitated transport of tryptophan and serotonin. In these carriers the counterions that can also coordinate to the Mn^{III} ion inhibit transport and the inhibition is roughly correlated to the magnitude of interaction, which is also reflected in the extent of ionic dissociation as determined by equivalent conductance measurements.

The kinetics of tryptophan and serotonin transport are first order in both substrate and carrier. The transport by equimolar mixtures of the individual interacting units (the Mn^{III} complex of the tetra-*tert*-butylsalphenveratrole tetradentate ligand and the benzo-18-crown-6 cyclic ether) shows some synergism. The two units, when covalently bound in the ditopic receptors, are considerably more effective and show ditopic cooperativity, which is moderate for tryptophan and considerably better for serotonin. The results correlate with molecular mechanics calculations and the relative energies associated with the optimized host-guest structures. The slower rate of serotonin transport is attributed to its greater hydrophilicity relative to tryptophan. Tritopic carriers that consist of two hydrophobic salphen units on either side of a dibenzo-18-crown-6 ether bridging unit are not efficient in the transport of tryptophan. This result, and the poor transport properties of the Mn-veratrole complex, have been rationalized in terms of either the blocking or unavailability of the crown ether unit in both of these ineffective carriers.

It is suggested that the interface-invading ability of the sterically unencumbered crown ether in the ditopic carriers lowers the kinetic barrier to interphase transport. The latter is thermodynamically driven by the concentration gradient between the source and receiving phase. The catalytic effect of the crown ether appendage is also apparent in the transport properties of ditopic carriers when alkali metal ions are present. In the latter case, transport is inhibited as the RNH_3^+ group of the tryptophan zwitterion competes with the alkali metal cations and does not have free access to the water-invading crown ether.

Experimental Section

General Remarks: Chemicals/Instrumentation

Details regarding the acquisition and purification of the solvents and reagents used, along with details regarding instruments used and spectroscopic techniques and methods can be found in the Supporting Information.

Synthesis

1,2-Dimethoxy-4,5-dinitrobenzene (1): A modified procedure of Frisch and Bogert[55] for the nitration of 1,2-dimethoxybenzene was carried out and the compound was obtained in 80% yield.[56]

1,2-Diamino-4,5-dimethoxybenzene (2): The reduction of 1,2-dimethoxy-4,5-dinitrobenzene was performed as reported by Weinberger and Day[57] and the product was obtained in 75% yield.

***N,N′*-4,5-Dimethoxybenzenebis(3,5-di-*tert*-butylsalicylideneimine), *t*Bu$_4$Veratrole (3):** Under an inert atmosphere, compound **2** (1.70 g, 10 mmol) was dissolved in MeOH (70 mL) to give a colorless solution. A solution of 3,5-di-*tert*-butylsalicylaldehyde (4.77 g, 20 mmol) in MeOH (50 mL) was added and the resulting bright yellow solution was refluxed for 18 hours. Upon cooling the product precipitated as a yellow crystalline material. The solid was collected by filtration in air and dried overnight under vacuum. Yield 4.2 g (70%).[56]

Nickel(II) *N,N′*-4,5-Dimethoxybenzenebis(3,5-di-*tert*-butylsalicylideneimine), *t*Bu$_4$NiVeratrole (4): Ligand **3** (3.00 g, 5 mmol) was dissolved in $CHCl_3$ (100 mL). Nickel acetate tetrahydrate (1.25 g, 5 mmol) was dissolved in 40 mL of methanol. This solution was slowly added to the solution of **3**. A bright red or orange powder precipitated immediately. Stirring was continued for one hour. The precipitate was collected by filtration, washed with EtOH (10 mL), and dried under vacuum overnight to yield an orange-red powder. Yield 2.96 g (90%). − $C_{38}H_{52}N_2NiO_4$ (659.55): calcd. C 69.41, H 7.66, N 4.26, Ni 8.93; found C 69.65, H 7.57, N 4.17, Ni 8.04. − UV/Vis (CH_2Cl_2): λ (ε × 10^{-3} м$^{-1}$ cm^{-1}) = 496 nm (br, 14.6), 466 (sh, 12.1), 404 (sh, 27.0), 386 (42.1), 371 (sh, 29.1), 298 (25.2), 266 (55.5). − IR (CsI): $\tilde{\nu}$ = 1614 cm^{-1} (vs, C=N), 383 (s). − ^{1}H NMR (300 MHz, CD_2Cl_2): δ = 7.99 (s, 2 H), 7.39 (d, 2 H), 7.26 (d, 2 H), 7.11 (d, 2 H), 4.00 (s, 6 H), 1.47 (s, 18 H), 1.32 (s, 18 H). − ^{13}C NMR (300 MHz, CD_2Cl_2): δ = 97.7, 120, 127, 131, 137, 138, 141, 150, 154, 164.

Manganese(III) *N,N′*-4,5-Dimethoxybenzenebis(3,5-di-*tert*-butylsalicylideneimine)X, *t*Bu$_4$MnVeratroleX [X = Cl (5) or I (6)]: A procedure similar to that described for the synthesis of **4** above was followed for the synthesis of **5** and **6**.[56]

4,5-Dinitrobenzo-18-crown-6 (7): Solid benzo-18-crown-6 (5 g, 16.0 mmol) was added slowly over thirty minutes to concentrated nitric acid (150 mL) with stirring. $CHCl_3$ (100 mL) was added to the yellow solution and the two layers were stirred for seven days. After this time the acid was diluted with an equal volume of distilled water. The product was extracted with chloroform (3 × 100 mL). The chloroform was evaporated to dryness leaving a yellow waxy residue. The product was used without further purification. Yield 5.5 g (85%). − ^{1}H NMR (300 MHz, [D$_6$]DMSO): δ = 7.76 (s, 2 H), 4.30 (m, 4 H), 3.76 (m, 4 H), 3.58 (m, 8 H), 3.50 (s, 4 H).

4,5-Diaminobenzo-18-crown-6 (8): Compound **7** (2 g, 4.95 mmol), 5% palladium on activated carbon (1 g), and methanol (100 mL) were placed into a hydrogenation vessel. The mixture was degassed and allowed to react with hydrogen gas at 40 p.s.i. with agitation for 18 hours. The solution was filtered under Schlenk conditions through a minimal pad of celite and the clear solution was reduced to dryness by removing the solvent under reduced pressure. A pale off-white powder was obtained that readily decomposed in solution when exposed to air but was moderately stable as a solid. The solid was stored under inert atmosphere conditions. Yield 0.85 g (50%).

4,5-Bis(3,5-di-*tert*-butylsalicylideneimine)benzo-18-crown-6, *t*Bu$_4$H$_2$18-C-6 (9): Under an inert atmosphere, compound **8** (1 g, 2.91 mmol) and 3,5-di-*tert*-butylsalicylaldehyde (1.36 g, 5.82 mmol) were dissolved in methanol (50 mL). The resulting solution was refluxed under N_2 for 48 hours. The product precipitated from solution upon cooling as a yellow powder and was isolated by filtration in air. Yield 3.25 g (72%).[56]

Nickel(II) 4,5-Bis(3,5-di-*tert*-butylsalicylideneimine)benzo-18-crown-6, *t*Bu$_4$Ni18-C-6 (10): An amount of nickel acetate tetrahydrate (0.16 g, 0.65 mmol) was dissolved in MeOH (50 mL) and added to a solution of **9** (0.5 g, 0.65 mmol) in CH_2Cl_2 (50 mL) resulting in an intense red solution. The solvent was slowly evaporated to afford fibrous red crystals. Yield 0.38 g (70%).[56]

Nickel(II) 4,5-Bis(3,5-di-*tert*-butylsalicylideneimine)benzo-18-crown-6·*n*-hexylammonium chloride, *t*Bu$_4$Ni18-C-6[HexNH$_3$Cl] (11): This compound was obtained in 40% yield in a manner analogous to that used for the synthesis of **10** in the presence of hexylammonium chloride.[56] The complex crystallized from a dark red MeOH/acetone solution upon slow evaporation of acetone.

[Nickel(II) 4,5-Bis(3,5-di-*tert*-butylsalicylideneimine)benzo-18-crown-6]AX, *t*Bu$_4$Ni18-C-6(AX) [AX = KI (12); CsI (13); 1/2 CsI (14)]: AX (0.60 mmol or 0.30 mmol in the case of **14**) was dissolved in MeOH (50 mL) and added to a solution of **10** (0.5 g, 0.60 mmol) dissolved in acetone (50 mL). The intense red color remained unchanged. The compounds **12**, **13** and **14** were obtained in yields of 80%, 85% and 85%, respectively.[56]

Manganese(III) 4,5-Bis(3,5-di-*tert*-butylsalicylideneimine)benzo-18-crown-6-X, *t*Bu$_4$Mn18-C-6X [X = Cl (15); I (16); B(Ph)$_4$ (17); Acetate (18); Pivalate (19)]: Manganese(II) acetate (0.16 g, 0.65 mmol) was dissolved in MeOH (50 mL) and added to a solution of **9** (0.5 g, 0.65 mmol) in $CHCl_3$ (50 mL), resulting in a dark brown solution. An excess amount of the sodium salt of the anion (2.6 mmol) was added to provide an anionic source for the Mn^{III} center. The ethanol solution of the compound was stirred in air overnight and the solvent removed. The residue was redissolved in chloroform (50 mL) and washed with deionized water (10 × 100 mL) to remove the excess salt and any sodium coordinated by the crown ether. The complex was isolated by evaporation of the remaining solvent. Crystals of **15** were obtained by slow evaporation of an ethanol or ethyl acetate solution of the complex.[56]

15: Yield 0.74 g (80%). − $C_{46}H_{64}MnN_2O_8Cl{\cdot}CH_3CH_2OH{\cdot}H_2O$: calcd. C 62.15, H 7.82, Mn 5.92, N 3.02; found C 61.88, H 8.14, Mn 5.87, N 3.09. − UV/Vis (CH_2Cl_2): λ (ε × 10^{-3} м$^{-1}$ cm^{-1}) = 483 nm (br, 12.2), 380 (20.5), 364 (sh, 19.7), 319 (20.9), 263 (30.4); UV/Vis (MeOH): λ (ε × 10^{-3} м$^{-1}$ cm^{-1}) = 459 nm (br, 12.1), 378 (29.7), 313 (24.0), 258 (35.5). − FAB-MS (3-nitrobenzyl alcohol): *m*/*z* = 827 [M − CH_3CH_2OH − H_2O − Cl]. − IR (CsI): $\tilde{\nu}$ = 1605 (vs, C=N) cm^{-1}, 393, 359. − Magnetic moment, μ_{eff}^{corr} = 4.41 BM/mole (300 K); 4.38 (4 K).

The syntheses and spectroscopic and physical properties of **16**, **17**, **18** and **19**, obtained in 95%, 87%, 95% and 94%, respectively, were similar to those of **15**.[56]

[Manganese(III) 4,5-Bis(3,5-di-*tert*-butylsalicylideneimine)benzo-18-crown-6 chloride]AX, *t*Bu$_4$Mn18-C-6Cl(AX) [AX = K, (20); KCl (21); CsI (22); CsCl (23); 1/2 CsCl (24)]: AX (0.60 mmol or 0.30 mmol in the case of **24**) was dissolved in methanol (50 mL) and added to a methanolic solution of **15** (0.61 g, 0.60 mmol). The compounds were isolated in 90%, 92%, 85% and 88%, respectively for **20**, **21**, **22** and **23**, by slow solvent evaporation.

[Manganese(III) 4,5-Bis(3,5-di-*tert*-butylsalicylideneimine)benzo-18-crown-6 iodide]AX, *t*Bu$_4$Mn18-C-6I(AX) [AX = KI (25); CsI (26);

Table 8. X-ray crystallographic and experimental data for complexes **11**−**15**, **27**

Complex	**11**[a]	**12**	**13**	**14**	**15**	**27**
Formula	$NiC_{52}H_{80}N_3O_8Cl$	$KNiC_{46}H_{66}N_2O_9I$	$CsNiC_{46}H_{64}N_2O_8I$	$CsNi_2C_{92}H_{128}N_4O_{16}I$	$MnC_{48}H_{72}N_2O_{10}Cl$	$CsMn_2C_{96}H_{144}N_4O_{20}ClI_2$
F.W. (g mol^{-1})	969.37	1015.74	1091.52	1923.24	927.51	2114.82
space group	$P2_1/n$	$P\bar{1}$	$P\bar{1}$	$P\bar{1}$	$P\bar{1}$	$C2/c$
a (Å)	10.58880(10)	10.37910(10)	10.0693(2)	18.818(4)	10.9387(2)	24.0961(6)
b (Å)	19.15051(10)	15.9553(2)	16.6268(1)	19.544(4)	14.3794(2)	30.2777(6)
c (Å)	30.9815(4)	18.449	19.2304(3)	20.335(4)	18.4478(4)	18.9944(4)
α (Å)	90	112.16	114.672(1)	106.57(3)	104.958(1)	90
β (Å)	93.7140(10)	102.97	102.098(1)	102.75(3)	104.245(1)	114.1030(10)
γ (Å)	90	96.43	93.290(1)	114.16(3)	99.140(1)	90
Z	4	2	1	2	2	4
V (Å^3)	6269.26(11)	2691.12(4)	2822.39	6033(2)	2639.45(8)	12649.6(5)
$\rho_{calcd.}$ (Mg m^{-3})	1.107	1.324	1.584	1.039	1.225	0.779
T (K)	158(2)	158(2)	173(2)	293(2)	173(2)	158(2)
λ (Å)	0.71073	0.71073	0.71073	0.71073	0.71073	0.71073
μ (mm^{-1})	0.502	0.690	1.860	1.370	0.358	0.829
$R1$[b] (all data)	0.0694	0.0734	0.0753	0.2170	0.0858	0.1725
$wR2$[c] (all data)	0.1755	0.2065	0.1758	0.3413	0.1570	0.4207

[a] See Table 1 for the numbering scheme of complexes. − [b] $R1 = \Sigma||F_o| - |F_c||/\Sigma|F_o|$. − [c] $wR2 = \{\Sigma[w(F_o^2 - F_c^2)^2]/\Sigma[w(F_o^2)^2\}^{1/2}$, $w = 1/[\sigma^2(F_o^2) + (0.0186P)^2 + 17.3751P]$, where $P = [\mathrm{Max}(F_o^2, 0) + 2F_c^2]/3$.

1/2 CsCl (27); 1/2 CsI (28)]: The synthesis of these iodo derivatives, in high yields, was also similar to that of **20**−**24**.[56]

Copper(II) 4,5-Bis(3,5-di-*tert*-butylsalicylideneimine)benzo-18-crown-6, *t*Bu$_4$Cu18-C-6 (29): This compound was obtained from copper acetate in a manner similar to that described for the synthesis of **10**.

4,4′,5,5′-Tetranitrodibenzo-18-crown-6 (30): Solid dibenzo-18-crown-6 (5 g, 13.9 mmol) was added slowly over thirty minutes to 150 mL of concentrated nitric acid and the mixture was stirred until all remaining solids dissolved. The orange solution was then poured over one liter of ice and a yellow solid precipitated. The solid was collected by filtration, washed with deionized water (100 mL), saturated sodium bicarbonate solution until there was no further CO_2 evolution, and then deionized water (3 × 100 mL). The yellow powder was allowed to air dry. Yield 7.2 g (96%). − ^{1}H NMR (300 MHz, [D$_6$]DMSO): δ = 7.73 (s, 4 H), 4.29 (unresolved, 8 H), 3.83 (unresolved, 8 H). − ^{13}C NMR (300 MHz, [D$_6$]DMSO): δ = 150.9 (4 C), 135.8 (4 C), 108.2 (4 C) 69.1 (4 C), 68.2 (4 C).

4,4′,5,5′-Tetraaminodibenzo-18-crown-6, (31): Compound **30** (2 g, 3.70 mmol) was ground to a fine powder and placed into a hydrogenation vessel along with one gram of palladium on activated carbon and distilled methanol (100 mL). The mixture was deoxygenated and allowed to react with hydrogen gas at about 40 p.s.i. with agitation for 18 hours. The solution was filtered under Schlenk conditions through a minimal pad of celite and the pale off-white filtrate was reduced to dryness with a cold trap. Compound **30** was obtained as a pale off white powder. The compound readily decomposed in solution when exposed to air, and was moderately stable as a solid. The material was handled under nitrogen and used immediately. Yield ≈50%.

4,4′,5,5′-Tetra(3,5-di-*tert*-butylsalicylideneimine)dibenzo-18-crown-6, (*t*Bu$_4$H$_2$)$_2$18-C-6 (32): Under an inert atmosphere, compound **31** (1 g, 2.38 mmol) and 3,5-di-*tert*-butylsalicylaldehyde (2.23 g, 9.52 mmol) were dissolved in methanol (50 mL). The solution was refluxed with stirring under N_2 overnight. The product precipitated from solution upon cooling as a yellow powder and was isolated by filtration in air. Yield 2.52 g (53%); m.p. 266−268 °C.

Bis[Manganese(III) 4,4′,5,5′-tetra(3,5-di-*tert*-butylsalicylideneimine)chloride] Dibenzo-18-crown-6, (*t*Bu$_4$Mn)$_2$18-C-6 (33): Manganese(II) chloride (0.10 g, 0.80 mmol) was dissolved in methanol (50 mL) and added to a solution of **32** (0.5 g, 0.39 mmol) in dichloromethane (50 mL). The resulting yellowish-brown solution was refluxed for eighteen hours with stirring under air. The solution was evaporated to dryness and the remaining dark brown residue was dissolved in acetone (50 mL). The brown solution was filtered and methanol (30 mL) was added to the filtrate. The resulting solution was allowed to evaporate to dryness to yield dark brown crystals of **33**. These were collected by filtration and dried under vacuum. Yield 70%.[56]

X-ray Crystallographic Study

Collection and Reduction of X-ray Data: Single crystal, X-ray diffraction data were collected for complexes **11**−**15** and **27**. For structures **11**, **12**, **13**, **15**, and **27** a selected crystal was attached to a glass fiber and mounted on the Siemens SMART system for data collection at 173(2)K (Mo-K_α radiation: λ = 0.71073 Å). Data collection and analysis procedures are described in the Supporting Information for each of the structures. Crystal and refinement data are listed in Table 8. Details concerning structure solution and refinement for each of the structures reported herein have been deposited as Supporting Information.

Acknowledgments

The authors gratefully acknowledge the support of this work by a grant from the National Science Foundation, CHE 9307382.

[1] P. Lauger, *Angew. Chem. Int. Ed. Engl.* **1969**, *8*, 42.
[2] [2a] L. R. DeYoung, K. A. Dill, *Biochemistry* **1988**, *27*, 5281−5289. − [2b] *Mammalian Amino Acid Transport Mechanisms and Control* (Eds.: M. S. Kilberg, D. Haussinger), Plenum Press, New York, **1992**. − [2c] M. S. Kilberg, B. R. Stevens, D. A. Novak, *Annu. Rev. Nutr.* **1993**, *13*, 137−165. − [2d] C. Seel, A. Ganan, J. de Mendoza, *Top. Curr. Chem*. **1995**, *175*, 101. − [2e] J. L. Sessler, A. Andrievsky, *Top. Curr. Chem.* **1996**, *176*, 1119.
[3] [3a] J. C. Skou, *Biochim. Biophysica Acta* **1957**, *23*, 394. − [3b] H. R. Kaback, E. R. Stadtman, *Proc. Nat. Acad. Sci. USA* **1966**, *55*, 920. − [3c] W. R. Penrose, G. E. Nichoalds, J. R. Piperno, D. L. Oxender, *J. Biol. Chem*. **1968**, *243*, 5921−5928.
[4] D. Rogers, *J. Bacteriol*. **1964**, *88*, 279.
[5] [5a] C. F. Fox, E. P. Kennedy, *Proc. Nat. Acad. Sci. USA* **1965**, *54*, 891. − [5b] T. H. D. Jones, E. P. Kennedy, *Federat. Proc*. **1968**, *27*, 644.
[6] C. Haskovec, A. Kotyk, *Europ. J. Biochem.* **1969**, *9*, 343.

[7] [7a] J. R. Piperno, D. L. Oxender, *J. Biol. Chem.* **1966**, 5732. – [7b] W. R. Penrose, G. E. Nichoalds, J. R. Piperno, D. L. Oxender, *J. Biol. Chem*. **1968**, *243*, 5921.

[8] O. H. Wilson, J. D. Holden, *J. Biol. Chem*. **1969**, *244*, 2737.

[9] K. Ring, *Angew. Chem. Int. Ed. Engl*. **1970**, *9*, 345−356.

[10] T. D. Brock, G. Moo-Penn, *Biochem. Biophysics* **1962**, *98*, 183.

[11] [11a] K. Maruyama, H. Tsukube, T. Araki, *Tetrahedron Letters* **1981**, *22*, 2001. – [11b] H. Tsukube, *Angew. Chem. Int. Ed. Engl*. **1982**, *21*, 304−305. – [11c] K. Maruyama, H. Tsukube, T. Araki, *J. Am. Chem. Soc*. **1982**, *104*, 5197−5203.

[12] J. P. Behr, J. M. Lehn, *J. Am. Chem. Soc.* **1973**, *95*, 6108.

[13] J. Rebek, Jr., B. Askew, D. Nemeth, K. Parris, *J. Am. Chem. Soc*. **1987**, *109*, 2432−2434.

[14] M. T. Reetz, J. Huff, J. Rudolph, K. Tollner, A. Deege, R. Goddard, *J. Am. Chem. Soc.* **1994**, *116*, 11588−11589.

[15] F. P. Rudkevich, J. D. Mercer-Chalmers, W. Verboom, R. Ungaro, F. de Jong, D. N. Reinhoudt, *J. Am. Chem. Soc.* **1995**, *117*, 6124−6125.

[16] Y. Aoyama, M. Asakawa, A. Yamagishi, H. Toi, H. Ogoshi, *J. Am. Chem. Soc*. **1990**, *112*, 3145−3151.

[17] H. Tsukube, S. Shinoda, J. Uenishi, T. Kanatani, H. Itoh, M. Shiode, T. Iwachido, O. Yonemitsu, *Inorg. Chem*. **1998**, *37*, 1585−1591.

[18] L. K. Mohler, A. W. Czarnik, *J. Am. Chem. Soc*. **1993**, *115*, 7037.

[19] [19a] M. Newcomb, R. C. Helgeson, D. J. Cram, *J. Am. Chem. Soc*. **1974**, *96*, 7367−7369. – [19b] M. Newcomb, J. L. Toner, R. C. Helgeson, D. J. Cram, *J. Am. Chem. Soc*. **1979**, *101*, 491−4947.

[20] [20a] K. Maruyama, H. Tsukube, T. Araki, *Tetrahedron Letters* **1981**, *22*, 2001−2004. – [20b] K. Maruyama, H. Tsukube, T. Araki, *J. Am. Chem. Soc*. **1982**, *104*, 5197−5203. – [20c] H. Tsukube, *Angew. Chem. Int. Ed. Engl*. **1982**, *21*, 304−305. – [20d] H. Tsukube, S. Shinoda, J. Uenishi, T. Kanatani, H. Itoh, M. Shiode, T. Iwachido, O. Yonemitsu, *Inorg. Chem*. **1998**, *37*, 1585−1591.

[21] [21a] S. Jonasdottir, C. G. Kim, J. Kampf, D. Coucouvanis, *Inorg. Chim. Acta* **1996**, *243*, 255−270. – [21b] S. M. Malinak, D. Coucouvanis, *Inorg. Chem*. **1996**, *35*, 4810−4811.

[22] [22a] D. T. Rosa, D. Coucouvanis, to be published. – [22b] D. T. Rosa, *Ph. D. Thesis*, University of Michigan, **1998**.

[23] F. C. J. M. Van Veggel, W. Verboom, D. N. Reinhoudt, *Chem. Rev.* **1994**, *94*, 279−299.

[24] [24a] D. N. Reinhoudt, J. A. A. de Boer, J. W. H. M. Viterwijik, S. Harkema, *J. Org. Chem*. **1985**, *50*, 4809. – [24b] A. R. van Doorn, R. Schaafstra, M. Bos, S. Harkem, J. van Eerden, W. Verboom, D. N. Reinhoudt, *J. Org. Chem*. **1991**, *56*, 6083−6094. – [24c] W. F. Nijenhuis, A. R. van Doorn, A. M. Reichwein, F. de Jong, D. N. Reinhoudt, *J. Am. Chem. Soc*. **1991**, *113*, 3607. – [24d] C. J. van Staveren, J. van Eerden, F. C. J. M. van Veggel, S. Harkema, D. N. Reinhoudt, *J. Am. Chem. Soc*. **1988**, *110*, 4494.

[25] [25a] N. Kobayashi, T. Osa, *Heterocycles*, **1981**, *15*, 675. – [25b] J. L. Sessler, T. D. Mody, R. Ramasamy, A. D. Sherry, *New J. Chem*. **1992**, *16*, 541−544.

[26] [26a] O. E. Sielcken, W. Dreuth, R. J. M. Nolte, Recl. Trav. Chim. Pays-*Bas.* **1990**, *109*, 425. – [26b] O. E. Sielcken, M. M. van Tilborg, M. F. M. Roks, R. Hendriks, W. Dreuth, R. J. M. Nolte, *J. Am. Chem. Soc*. **1987**, *109*, 4261. – [26c] Z. Gasyna, N. Kobayashi, M. J. Stillman, *J. Chem. Soc., Dalton. Trans.* **1989**, 2397. – [26d] N. Kobayashi, A. B. P. Lever, *J. Am. Chem. Soc*. **1987**, *109*, 7433. – [26e] N. Kobayashi, Y. Nishiyama, *J. Chem. Soc., Chem. Commun.* **1986**, 1462.

[27] S. Can, O. J. Bekaraglou, *J. Chem. Soc., Dalton Trans.* **1988**, 2831.

[28] A. Gul, A. I. Okur, A. Cihan, N. Tan, O. Bekaroglou, Synth. React. Inor. Met.-*Org. Chem*. **1986**, *16*, 871−884.

[29] [29a] S. Karabocek, N. Karabocek, *Polyhedron* **1997**, *16*, 1771−1774. – [29b] Y. Gok, I. Degirmencioglu, S. Karabocek, *Synth. React. Inor. Met.-Org. Chem*. **1997**, *27*, 331−345.

[30] [30a] D. T. Rosa, D. Coucouvanis, *Inorg. Chem*. **1998**, *37*, 2328. – [30b] D. T. Rosa, V. G. Young, D. Coucouvanis, *Inorg. Chem*. **1998**, *37*, 5042−5043.

[31] J. R. Cooper, F. E. Bloom, R. H. Roth, *The Biochemical Basis of Neuropharmacology*, Oxford University Press, Oxford, **1996**.

[32] R. M. Silverstein, G. C. Bassler, T. C. Morrill, *Spectrometric Identification of Organic Compounds*, John Wiley & Sons: New York, **1991**; 5th ed.

[33] S. D. Bella, I. Fragala, M. A. Diaz-Garcia, I. Ledoux, T. J. Marks, *J. Am. Chem. Soc*. **1997**, *119*, 9550−9557.

[34] A. Van der Bergen, K. S. Murray, M. J. O'Connor, B. O. West, *Aust. J. Chem*. **1969**, *22*, 39.

[35] D. Christodoulou, M. G. Kanatzidis, D. Coucouvanis, *Inorg. Chem*. **1990**, *29*, 191−201.

[36] O. Nagano, A. Kobayashi, Y. Sasaki, *Bull. Chem. Soc. Jpn*. **1978**, *51*, 790−793.

[37] P. Seiler, M. Dobler, J. D. Dunitz, *Acta Cryst*. **1974**, *B30*, 2744.

[38] C. J. Pedersen, *J. Am. Chem. Soc.* **1970**, *92*, 386.

[39] K. V. Domasevitch, V. V. Ponomareva, E. B. Rusanov, *J. Chem. Soc., Dalton Trans.* **1997**, 1177−1180.

[40] J. E. Davies, B. M. Gatehouse, K. S. Murray, *J. Chem. Soc., Dalton Trans.* **1973**, 2523.

[41] D. L. Ward, S. B. Dawes, O. Fussa, J. L. Dye, *Am. Cryst. Assoc., Abstr. Paper (Winter)* **1985**, *13*, 25.

[42] The flux values (Table) used for comparison purposes was calculated using the 24 h measurement and is expressed in mol or equivalents and dividing by: the time (in seconds), number of mol of carrier, and the area of $2.2 \times 10^{-3} m^2$. This value was then multiplied by 10^4 to give a reasonably scaled number.

[43] [43a] D. T. Rosa, Dissertation Thesis, University of Michigan, **1998**. – [43b] D. T. Rosa, D. Coucouvanis, manuscript in preparation.

[44] [44a] T.M. Fyles, in *Inclusion Aspects of Membrane Chemistry* (Eds. Y. Osa, J. Atwood), Lluwer: Dordecht, **1991**, Vol. 2, pp. 59−110. – [44b] B. D. Smith, S. Gardiner, *Advances in Supramolecular Chemistry*, **1999**, *5*, 157−202.

[45] M. F. Paugam, J. T. Bien, B. D. Smith, *J. Am. Chem. Soc*. **1996**, *118*, 9820−9825.

[46] The similarity is apparent in the ^{1}H NMR spectra of ligands **3** and **9**. The aromatic protons of **3** appear at δ = 8.71, 7.44, 7.28, and 6.87, and those of **9** at δ = 8.68, 7.43, 7.25, and 6.85. The electronic spectra of **6** and **16** also are very similar.

[47] D. J. Cram, R. N. Trueblood, *Top. Curr. Chem*. **1981**, *98*, 43.

[48] D. J. Cram, J. M. Cram, *Acc. Chem. Res.* **1978**, *11*, 8.

[49] C. J. Pedersen, *Angew. Chem. Int. Ed. Engl*. **1988**, *27*, 1021−1027.

[50] K. Ring, *Angew. Chem. Int. Ed. Engl*. **1970**, *9*, 345−356.

[51] [51a] A. R. Oki, D. J. Hodgson, *Inorg. Chim. Acta* **1990**, *170*, 65−73. – [51b] J. W. Gohdes, W. H. Armstrong, *Inorg. Chem*. **1988**, *27*, 1842−1846.

[52] D. T. Rosa, D. Coucouvanis, to be published.

[53] The program Hyperchem was used for performing mm+ calculations. We feel that the absolute values of the energies obtained for the optimized structures are rather unreliable given the lack of sophistication in these calculations. The relative values of the energies, however, can be used for comparative purposes. These are as follows: carrier with tryptophan interacting with the H_2O, 59.67 kcal/mol; carrier with tryptophan interacting with the metal, 73.3 kcal/mol; carrier with serotonin interacting with H_2O, 31.4 kcal/mol; carrier with serotonin interacting with the metal, 27.2 kcal/mol.

[54] *The Merck Index, 11th Ed.* (Ed.: S. Budavari), Merck & Co., Rahway, NJ, **1989**.

[55] J. Frisch, M. T. Bogert, *J. Org. Chem.* **1943**, *8*, 331.

[56] The detailed synthesis, spectroscopic characterization and analytical data for the compound(s) have been deposited as Supporting Information.

[57] L. Weinberger, A. R. Day, *J. Org. Chem*. **1959**, *24*, 1451−1455.

Received August 30, 2000
[I00351]